2018

The effect of metformin on absolute telomere length

Robb-Mackay, Cameron

The Effect of Metformin on Absolute Telomere Length

Written by: Cameron Robb-MacKay

Committee Members: Dr. David Law (co-supervisor), Dr. Carney Matheson (co-supervisor) and Dr. Michael Rennie

External Reviewer: Dr. Lea Harrington

Thesis submitted for the Masters of Science degree in Biology

Department of Biology

Lakehead University, Thunder Bay, Ontario, Canada

Declaration:

I hereby declare that this submission is my own work and that, to the best of my knowledge and belief, it contains no material previously published or written by another person, except where due acknowledgment has been made in the text.

Cameron Robb-MacKay

Contents

Table of Figures

Table of Tables

Abstract:

In this study, the relationship between average absolute telomere length and metformin use was examined. Human blood samples were obtained from 106 participants ranging from 42-100 years old. Samples were split into four cohorts for analysis: non-type 2 diabetics not taking metformin (Cohort 1), type 2 diabetics taking metformin (Cohort 2), type 2 diabetics not taking metformin (Cohort 3), and non-type 2 diabetics taking metformin. DNA from blood samples were extracted and purified using an and average absolute telomere length was measured using quantitative polymerase chain reaction (qPCR). The average absolute telomere length increased with age for Cohort 2 samples and decreased slightly with age for Cohort 1 samples. This led to the mean average absolute telomere length of Cohort 2 beginning as a lower value than Cohort 1 and then matching and later surpassing the Cohort 1 levels with increased age. This trend was intriguing but showed no statistical significance between the mean average absolute telomere length for Cohort 1 and Cohort 2. Cohort 3, however, had a mean average absolute telomere length which was considerably lower than Cohort 1 and 2. The difference between Cohort 3 and 1 and Cohort 3 and 2 was statistically significant between the ages of 71-80. This lower average absolute telomere length in Cohort 3 when compared to Cohort 2 indicates that metformin use may reduce telomere shortening in older adults. Overall, the findings provide further evidence of metformin's geroprotective effects, and indicate the need for further, more in depth studies in the future with a larger sample size.

Acknowledgments:

I would like to thank the Principle Investigator of this project Dr. Chris Lai for his assistance designing the project as well as promoting the project and providing funding and research for the research. I would also like to thank the following people who assisted with obtaining the blood samples, Savannah Prete, Lisa Stein, Susan Thomson, and Stacy Davidson. I would also like to thank Dr. Mario Nucci for his contribution in developing the project and also for providing resources and funding for the project. I would also like to thank Ryan Lehto and Neil Esau for granting me the use of the facilities at CG labs. I would also like to thank the Northern Ontario Academic Medical Association for funding this research and the Research Ethics Board of Lakehead University for providing permission to undertake this research. I would also like to acknowledge the invaluable help of my committee members, co-supervisors Dr. David Law and Dr. Carney Matheson, and Dr. Michael Rennie, as well as my external reviewer Dr. Lea Harrington.

1: Literature Review/Introduction

For as long as humans have been aware of their own mortality, they have yearned for a greater understanding of the aging process and possible remedies for this invisible illness. Despite the fascination of many, the 'how's' and 'why's' of aging had remained a mystery for millennia. From Ponce de León's epic voyage to the new world in search of the fabled 'Fountain of Youth', to Countess Elisabeth Báthory's macabre ritual of bathing in virgin blood with the aim of retaining her beauty and virility, mankind's journey to cultivate a greater understanding of the aging process has been a long and storied one. With the dawn of the 20th century and the veritable Cambrian explosion of paradigm-shifting scientific discoveries that soon followed, humankind's knowledge began to expand - if only modestly. It became well documented that the aging process had several intersecting etiologies, all with differing degree of impact from individual to individual. Later, genetics became well established as playing an important role in how one aged. However, knowledge about the impact of epigenetics and environmental factors were also found to be invaluable.

Pharmacological studies looking for methods of mitigating the effects of aging were also undertaken. Eventually, the antihyperglycemic drug, metformin, used primarily to treat symptoms of type 2 diabetes, was examined and was found to show promising anti-aging properties. Although this geroprotector may have initiated many studies to investigate its effectiveness at treating various diseases, little has been done to examine its role in preventing DNA degradation, particularly telomere reduction, that could lead to aging.

This study aims to examine the role metformin has on human telomeres, the protective caps which protect DNA from degradation over time. It is conducted with the aim to continue in

furthering our knowledge of the aging process and potentially lead to notable revelations in the future.

1.1 Use of metformin in type 2 diabetes therapy

Currently, metformin is the most widely prescribed drug to treat hyperglycemia for individuals with type 2 diabetes (1). It is estimated to be prescribed to over 120 million people worldwide (1). Type 2 diabetes, also referred to as non-insulin dependent diabetes or adult-onset diabetes, encompasses those who have insulin resistance and relative (as opposed to absolute) insulin deficiency (48). It is the most common form of diabetes, making up 90-95% of all cases (48). People with type 2 diabetes have elevated levels of blood glucose, and since they do not have insulin levels to match this increased amount of glucose, their insulin secretion is said to be defective and insufficient to compensate for insulin resistance (48). Metformin treats type 2 diabetes by increasing sensitivity to insulin, specifically in the liver (46). It also functions as a caloric restrictor, reducing the amount of glucose taken in the body.

1.2 Metformin development and history

Metformin, also known as dimethylbiguanide (Figure 1), is an oral antihyperglycemia drug that has over recent decades become the primary treatment for type 2 diabetes. Origins of the drug begin with the precursor plant *Galega officinalis* L. which was a traditional herbal remedy used to treat worms, epilepsy (‘falling-sickness’), fever, and pestilence (49). The herb was eventually found to contain high concentrations of guanidine, a chemical that was soon realized to be effective in lowering blood glucose levels (49).

In 1922, Werner and Bell chemically synthesized dimethylbiguanide (Figure 1), later called metformin (50). It was seven years later, in 1929, when its glucose-lowering properties were discovered (49). In the 1940s, metformin was discovered to be an effective treatment against malaria and influenza (49). In 1957, Jean Sterne, a physician at Aron Laboratories in France investigated the effect metformin had on both type 1 and type 2 diabetics (49). He found that in some type 2 diabetics, metformin use would negate the need for insulin treatments, while lowering the necessary dosage requirements for other type 2 diabetic patients (49). However, these promising results were exclusive to type 2 diabetics, with type 1 diabetic patients still requiring insulin treatments (49). Metformin ultimately had relatively low prescription rates due to being weaker than other glucose-lowering biguanides (49).

However, by the 1970s many in the biguanide family, such as phenformin (Figure 1), were found to be linked to lactic acidosis and were discontinued from clinical use (49). Studies looking at the risk of lactic acidosis from metformin use found the incidence to be considerably lower than other biguanides and attributed most cases of lactic acidosis to contraindicated use (51, 52). Also, in some studies it was debatable whether incidences of lactic acidosis with metformin were greater than background rates for type 2 individuals (49). Although taking metformin was not found to be a significant risk for the development of lactic acidosis, the association with the notorious biguanide family resulted in plummeting prescription rates, driving metformin into relative obscurity (49).

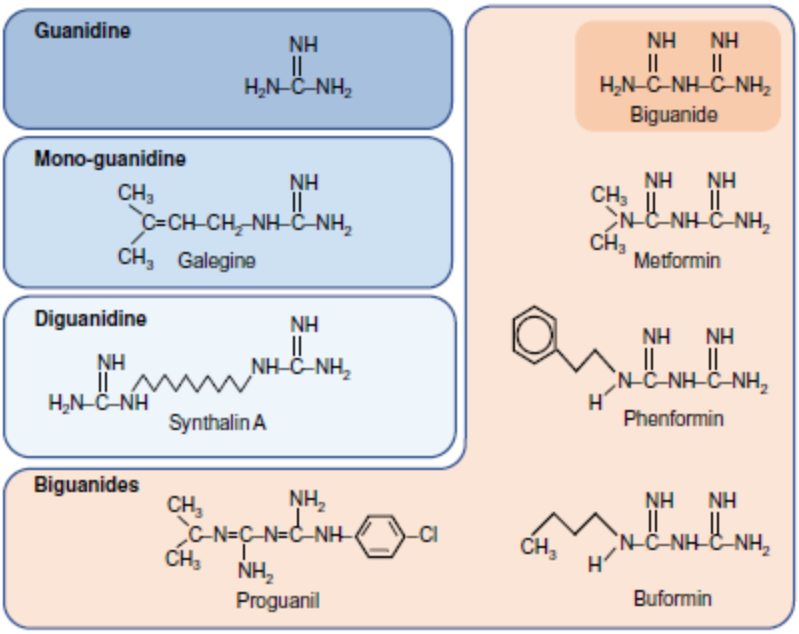

Figure 1: The structure of biguanide and other related compounds including Metformin (49).

A resurgence of research in the 1980s and early 1990s resulted in the development of fixed-dose combinations of metformin with sulfonylureas, as well other classes of oral glucose-lowering agents (49). The unique benefits and usefulness of metformin, discovered through this research, led to the drug being approved for therapeutic use in Canada in 1972 (53). In 1995 it received FDA approval for use in the United States (49). A long-term retrospective study in the UK in 1998 cemented metformin as the preferred initial therapy to manage type 2 diabetes-related hyperglycaemia (49). The study noted that, alongside its glucose-lowering effects, metformin had the benefit of weight neutrality, low hypoglycemia risk, and reduced cardiovascular risk (49, 54). Because of these benefits, its extensive history of clinical use, and a possible reduction of cancer incidence, metformin is currently globally recognized as the first-line of oral therapy treatment for type 2 diabetes (55, 56, 57, 58).

1.3 Metformin molecular action and effects

Due to its similarity to other biguanides, yet uniqueness in being a considerably safer treatment, there has been a great deal of interest in deciphering the drug's mechanism of action. Currently, researchers are still in the process of uncovering all the therapeutic biochemical mechanisms initiated by the drug. These processes are difficult to definitively attribute to metformin, as it passes through many regions of the mammalian anatomy and interacts with multiple biochemical pathways during the organism's anatomical lifespan. Supra-pharmaceutical levels of metformin are required to achieve the desired therapeutic effects for type 2 diabetics, strongly supporting the notion that the therapeutic effects are not solely attributed to the modification of a single/specific protein target (55).

The pathway of orally administered metformin passes through a number of organs within the body before its elimination (Figure 2). Orally administered metformin is absorbed by enterocytes in the apical membrane of the intestine via the plasma monoamine transporter (PMAT) and organic cation transporter 3 (OCT3) (59). It exits these cells via the organic cation transporter 1 (OCT1) molecule of the basolateral membrane (59). Next, metformin is delivered to the liver via the portal vein where it is taken up by the hepatocytes (59). It enters the hepatocytes via the OCT1/3 molecules and is excreted into the bloodstream and bile through the multidrug and toxin extrusion 1 (MATE 1) transporter molecule (59). Lastly, metformin reaches the kidneys, entering the renal epithelial cells through the organic cation transporter OCT2 transporter molecule (59). It is eliminated from the renal epithelial cells unchanged via the MATE transporter molecules (59).

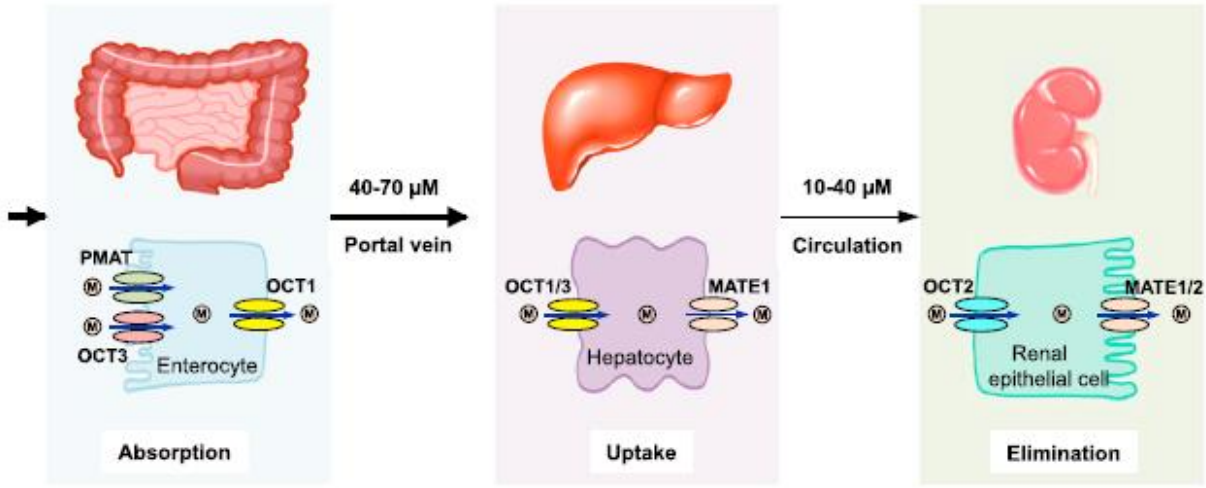

Figure 2: The path of orally administered metformin through the body and biochemical interactions (59).

It is widely accepted that metformin is able to lower glucose levels in the body through the stimulation of adenosine monophosphate-activated protein kinase (AMPK), an essential cellular energy sensor and regulator (59). The AMPK is a multi-subunit enzyme that regulates lipid biosynthetic pathways through the phosphorylation and inactivation of various key enzymes such as acetyl-CoA carboxylase (ACC) enzyme (60). The AMPK's regulatory effects are able to stimulate Adenosine Triphosphate (ATP)-producing catabolic pathways (glycolysis, fatty acid oxidation, and mitochondrial biogenesis) and to inhibit ATP-consuming anabolic processes (gluconeogenesis, glycogen, fatty acid, and protein synthesis). Metformin's stimulation of AMPK can cause a reduction in glucose levels by promoting hepatic gluconeogenesis, increasing liver insulin sensitivity, increasing muscle glucose transport, decreasing the amount of plasma glucose and triglycerides, and increasing fatty acid oxidation in the adipose tissue (2, 21). The action of AMPK is also able to inhibit glycogen synthase, reducing the production of glycogen (21).

In the liver, AMPK is able to partially inhibit gluconeogenesis by phosphorylating the CREB-binding protein (CBP) (21). Protein kinase C initiates the dissociation of the gluconeogenic CREB-CBP (CREB binding protein)-TORC2 (transducer of regrulated CREB 2) transcriptional complex, resulting in a chain reaction that causes the transcriptional machinery to be disassembled and the enzyme genes essential for gluconeogenesis, phosphoenolpyruvate carboxykinase (PEPCK) and glucose-6-phosphatase (G6Pase) to have their expression inhibited (21).

The activation of AMPK by metformin has also been shown to affect lipid and cholesterol synthesis in the liver, muscle and adipose tissues by decreasing both fatty acid synthase (FAS) expression and activating malonyl-CoA carboxylase (21). These desired results can be obtained indirectly by the inactivation of ACC and 3-hydroxy-3-methylglutaryl (HMG)-Co reductase (21). Furthermore, the action of AMPK is able to inhibit adipogenesis through the inhibition of the activity of sterol regulatory element-binding protein-1c (SREBP-1c), a transcription factor that is essential for fatty acid synthesis (21). Stimulation of AMPK is also able to increase glucose uptake in the skeletal muscles by inducing the enzyme hexokinase II expression and upregulating the transcription of the GLUT4 (glucose transporter type 4) gene (21).

There are also other AMPK-independent pathways that have been suggested as mechanisms of action of metformin, such as activating changes in the gut or intestinal microbiota. The intestines also play an important role in metformin's glucose-lowering effect by facilitating uptake and utilization of glucose (3, 4). Metformin can also act on MAPK- and PKA-dependent mechanisms as an alternative to mechanisms that utilize AMPK (22). Metformin's ability to decrease cyclic adenosine monophosphate (cAMP) production inhibits catecholamine-

stimulated lipolysis, reducing both MAPK- (Mitogen-Activated Protein Kinases -) and PKA- (Protein Kinase K-) dependent activities (21). In addition, adiponectin is also activated by metformin and can further stimulate AMPK to reduce hepatic lipid accumulation by both increasing β-oxidation and decreasing *de novo* synthesis of fatty acids (21).

Together, these combined molecular effects are able to result in an overall slowing of the aging process and an extension of longevity. Every year, more and more knowledge is generated about metformin's various biochemical mechanisms (Figure 3). Although a better understanding of how metformin affects the human body is beginning to take form, more research is still required to better understand the minutia of these internal biochemical processes.

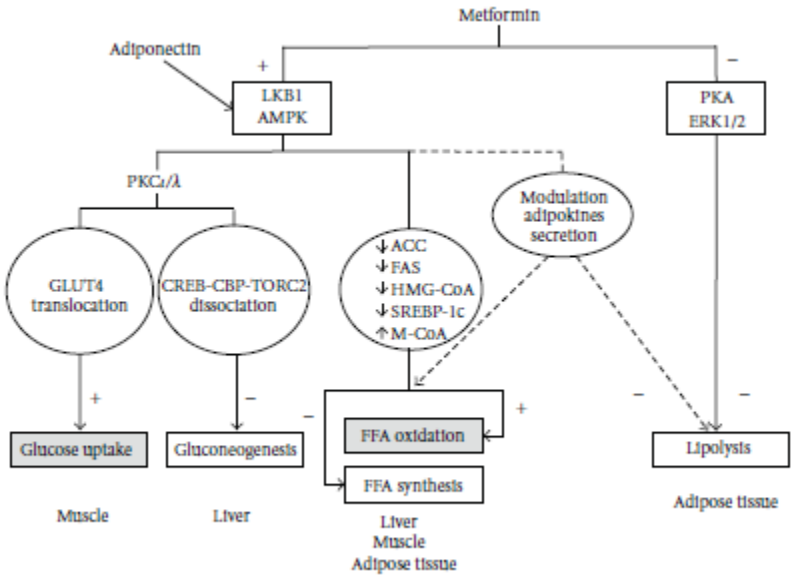

Figure 3: A visual summary of metformin's antihyperglycemic effects (21).

1.4 Alternate uses for metformin

Because comorbidity is frequently found with cancer and type 2 diabetes, there has been a great deal of research looking into metformin's effect on various forms of cancer. Insulin and insulin-like growth factor 1 (IGF-1) play an important role in regulating cell survival and mitogenesis (61). Both these growth factors are present in cancers of the breast, liver, colon, pancreas, and skin, hinting at the possibility of metformin to reduce the cancerous growth patterns associated with these stimuli (62). This possibility is further supported by evidence showing that caloric restriction (CR) can reduce IGF-1 activity, simultaneously reducing the incidence of cancer in *in vivo* animal models (63).

Several studies have examined metformin's effect on cancer, and the majority of evidence indicates that metformin treatments have the potential to reduce mortality rates and improve longevity for patients affected by breast, liver and ovarian/endometrial cancers (61, 66, 67). Other studies have shown that metformin treatments may be beneficial for individuals with colorectal, pancreatic or prostate cancer (61, 64, 65). A comprehensive meta-analysis by Franciosi *et al*. (68) examined the relationship between metformin use and overall mortality and found that there was an overall 35% reduction in cancer mortality rates observed in patients taking metformin. Furthermore, metformin has also shown to improve the effectiveness of chemotherapy while reducing some of the side effects (61, 69, 70).

Metformin has also been shown to be a useful preemptive treatment for individuals diagnosed with prediabetes (71). Alongside lifestyle changes, early metformin treatment was found to be effective in the prevention of type 2 diabetes (71). It should be noted that lifestyle changes were found to have a greater impact as a preventative measure than the metformin treatments (71). Similarly, metformin was also shown to be moderately beneficial for treating obesity, yet lifestyle changes were still found to be more effective overall (72).

There have been many studies looking at the benefits of metformin therapy to treat polycystic ovary syndrome (PCOS) as insulin resistance and hyperinsulinemia have been shown to contribute to the condition (73). Hyperinsulinemia initiates hyperandrogenism, which leads to anovulation and infertility (73). It has been found that metformin is quite effective in reversing the metabolic abnormalities associated with PCOS leading to the establishment of regular menstrual cycles and improved fertility (73, 74).

Metformin use has also been shown to be beneficial in improving cardiovascular health. Use of metformin has been shown to normalize blood pressure, improve the metabolic risk factor profile, and increase the fibrinolytic activity in individuals with hypertension (75). Overall, metformin therapy has been found to reduce the risk of cardiovascular-related morbidity and mortality (76).

1.5 Metformin's effect on lifespan in animal models

Metformin's wide range of health benefits and diverse biochemical pathway interactions has led to a great deal of interest in its effects on lifespan and the aging process(es). Currently, much of the aging research available on metformin has existed through studies of animal models.

Metformin treatment increased lifespan in several mice studies. It improved health and lifespan in male mice, where long-term treatment with metformin (0.1% w/w in diet) starting at middle age was effective in increasing mean lifespan by around 6% (9). However, a higher dose (1% w/w diet) was toxic to the mice, shortening mean lifespan by 14% (9). This is likely due to lactic acidosis, as high doses of metformin have been associated with its development (10). Low doses of metformin gave the mice increased sensitivity to insulin, reduced low-density lipoprotein (LDL) and cholesterol levels without a decrease in caloric intake, and improved

physical performance. The lack of decrease in caloric intake is important because it shows that any results found were not a result of CR. These results mimic the benefits of CR, which suggest that metformin acts in a similar way with respect to its benefits in extending lifespan and health, and suggest that metformin prevents the onset of metabolic syndrome. At the molecular level, metformin increased antioxidant protection and AMPK activity, reducing chronic inflammation and overall oxidative damage accumulation (9). In the study by Martin-Montalvo *et al*. (9) the serum level of metformin was found to be one order of magnitude higher than what is found in diabetics on metformin, so the effects of this drug may be less pronounced in people taking metformin as they may not receive a high enough dose to realize the increased health and lifespan benefits (9).

Metformin may need to be taken from a young age to fully realize its anti-aging effects. In a study done on female SHR mice, the mean lifespan of the mice was increased significantly when treatment with metformin was initiated at a young age, insignificantly at middle age, and not at all at an older age (11). The treatment that started at the age of three months increased mean lifespan by 14% and maximum lifespan by 1 month (11). The treatment started at 9 months only increased mean lifespan insignificantly by 6%, while the treatment started at 15 months failed to increase mean lifespan at all (11). If this mouse model holds true in humans, this suggests that treatment with metformin over a longer period of time can affect lifespan but would not be as effective if started later in life, which is often when most people begin to think about the consequences of aging (11). Another study performed on female SHR mice corroborated these results. Compared to control mice, mice receiving daily 100 mg/kg treatments of metformin had mean lifespan increase by 38%; the mean life span for the last 10% of survivors increased by 21%, and maximum life span increased by 2.8 months (+10%)(12).

Similarly, in two other studies done on female HER-2/neu mice, metformin increased mean lifespan by 4-8%, and increased the maximum lifespan by 1 month (13, 14). The increase in lifespan was attributed to the inhibition of mammary tumor development (13, 14). Metformin treatment was initiated at 2 months of age, which compared to the studies mentioned above is a relatively young age (13, 14).

In a study done on 129/Sv mice given 100 mg/kg daily for 24 months, females had a 5% increase in mean lifespan while males had a 13% decrease (15). This was the first study that showed a difference in metformin's effect on males versus females, which is an important factor as most of the mouse studies mentioned here were done on female mice. The authors suggested two possible reasons for this difference: fundamental differences in the mechanisms of aging in females and males and/or that the target of metformin is different in females versus males (15).

Regardless of sex-related differences in mammalian response to metformin treatment metformin's effects appear to apply to other animal clades as well. Metformin has been shown to increase health and extend median lifespan in *C. elegans* L. in a similar mechanism as CR, independent of the insulin-signaling pathway (16). Metformin slowed locomotory decline in nematodes, suggesting that metformin can promote or extend youthful physiology (16). The authors demonstrated that metformin acts as a CR mimetic by showing that in a nematode strain that induces CR, metformin does not further increase the benefits of a CR diet, but instead shows a negative impact on lifespan (16). This is likely due to both CR and metformin treatment together being too extreme to be beneficial. Also, metformin treatment showed delayed egg-laying, decreased age pigment levels, reduced progeny production and decreased fat, all of which are indicators of CR (16). This study also investigated the biochemical roles of the energy sensor AMPK and the AMPK-activating kinase LKB1 (liver kinase B1), which were both activated by

metformin (16). Both AMPK and LKB1 were found to be essential for improving health benefits of *C. elegans*, suggesting a conserved metabolic loop across various phyla (16). The study also found that the transcription factor SKN-1 plays an essential role in the extension of health in *C. elegans* (16). SKN-1 functions in nematode sensory neurons to promote dietary restriction longevity benefits and in intestines, helping to improve resistance to oxidative stress (16). In order for metformin-mediated health expansion to occur, SKN-1 must be expressed in both the neurons and the intestines, lending support to the notion that that metformin functions as a middle-age geroprotector through the regulation of CR metabolism and anti-oxidant defenses (16). These revelations about SKN-1 can become pharmacologically important when applied to the orthologous nuclear respiratory factor (Nrf) mammalian transcription factors Nrf1 and Nrf2, which are able to activate genes encoding phase 2 detoxification enzymes (16). The Nrf2 confers several defensive health-promoting effects in mammals and may be able, through the use of metformin, to combat neurodegeneration, chronic inflammation, and cancer in mammals (16).

Another study done by Cabreiro *et al*. (17) showed that metformin may slow aging in nematodes by regulating their gut microbial folate and methionine metabolism. This finding raises the possibility that metformin might therefore also influence mammals by affecting their microbial metabolism or composition by promoting a better balance of gut microbiota species (17). They found that metformin at doses of 25, 50, and 100 mM increased the mean lifespan of *C. elegans* by 18%, 36%, and 3%, respectively (17). Both studies above noted that metformin increases lifespan via AMPK-dependent activation of SKN-1, but the Cabreiro *et al*. (17) study concluded that this is because they promote resistance to biguanide toxicity (16, 17). Both studies noted that as the concentration of metformin is increased, there is a point in which the effects become detrimental and actually shorten lifespan, which is likely due to drug toxicity.

Both studies discovered that when a CR diet was induced, metformin had the opposite effect and shortened lifespan (16, 17).

Overall, the research data on metformin gathered from animal models provides some intriguing revelations. It seems that the most animal models indicate the importance of biological sex as well as age of treatment initiation in determining metformin's effect on aging and longevity. Interestingly, evidence may also indicate that a CR diet taken alongside metformin may negate some of the drug's anti-aging properties. This is a point of interest as it has been demonstrated that lifestyle changes such as CR diets undertaken simultaneously with metformin treatments are the most effective for preventative treatment of type 2 diabetes (71). It has also been shown that metformin use, combined with a CR diet, led to additive health benefits as opposed to worsened outcomes (20). Perhaps this difference could be indicative of specific differences in the way metformin affects biochemical pathways. Other evidence that points to metformin's diversity in biochemical influence comes from the fact that higher doses in mice models resulted in lifespan shortening, while in humans supra-pharmaceutical doses are required to be effective (9). The vastly different outcomes between mouse and human responses to large doses could be due to high doses of metformin in mice may cause lactic acidosis, while the risk for lactic acidosis in humans with high does is low (10, 49, 51, 52, 55). These findings indicate the delicate balance required to provide optimal therapeutic treatment with metformin.

1.6 Metformin mimics caloric restriction

Metformin has been described as a geroprotector, which is a drug that decreases the rate of aging and therefore extends lifespan. The main explanation for metformin's lifespan increasing benefits is that it is a CR mimetic (5). Caloric restriction is simply restriction of food

intake, which results in a restriction in the intake of energy. Caloric Restriction extends lifespan by delaying or slowing the aging process (5). Specifically, evidence suggests that maximum lifespan can be increased through CR and, therefore, through metformin usage as can be seen in the *Drosophilia melanogaster* L. model (24).

Excessive caloric intake can lead to obesity that in turn can increase the instance of age-related ailments such as diabetes, atherosclerosis, thrombosis, hypertension, various forms of cancer, coronary heart disease, stroke, osteoporosis, and Alzheimer's disease (23). Since caloric intake is so closely related to age-related diseases, it can be logically concluded that drugs that mimic CR could in turn regulate the aging process (23).

Caloric Restriction has shown health benefits in flies, rodents, monkeys, and humans. In many animal models, it has been shown to extend mean and/or maximum lifespan, as well as delay age-related physiological changes or age-related diseases such as type 2 diabetes. It has been shown to have effects on the insulin and IGF-1 signaling systems, as well as altering the activity of transcription factors such as AMPK and TOR (target of rapamycin) (6). The insulin/IGF-like signaling (IIS) and nutrient response pathways, which are defined by the mechanistic target of rapamycin (mTOR), control aging and age-associated pathology in worms, insects, yeast, and mammals (7, 8).

Further benefits have also been shown by implementing additional CR alongside use of metformin (20). In a study examining male OLETF rats with initial ages of 20 weeks, subjects were given daily doses of 300 mg/kg for 12 weeks (20). Both metformin treatment and CR diets were found to cause decreased adiposity in the rats (20). The combination of CR and metformin treatment provided more effective post-challenge glucose tolerance (20). The combination treatment also reduced levels of serum alanine aminotransferases, resulting in lowered liver

triglyceride levels which could lead to improved conditions for nonalcoholic fatty liver disease (NAFLD) (12). The combination treatment of CR and metformin reduced the levels of the hepatic lipogenesic ACC and stearoyl-CoA desaturase-1 (SCD-1) (20) and increased the amount of hepatic mitochondrial activity (shown through the increased levels of β-hydroxyacyl CoA dehydrogenase (β-HAD)) (20). Overall, this indicates that therapeutic metformin treatment and CR independently improve glycemic control and NAFLD outcomes and likely act via different biochemical pathways (20).

1.7 Metformin may reduce oxidative damage

Through the body's use of oxygen, potentially deleterious reactive oxygen metabolites, such as superoxide, ozone and hydrogen peroxide (H_2O_2) are generated (24). An overabundance of these oxygen molecules can lead to an aging process known as oxidative stress (24). Over time, the imbalance between prooxidants and antioxidants will result in enough oxidative stress to produce oxidative damage in molecules such as carbohydrates, nucleic acids, lipids, and proteins and thus alter their structure and impair their functions (24, 75). The degree of oxidative damage increases with age and is believed to be the major cause of cellular senescence and is considered to be one of the modalities of aging (24).

Many studies have shown that oxidative damage can be mediated via CR, further suggesting that CR can counteract the aging process (24). Caloric Restriction reduced the metabolic rate of Fischer rats if CR treatments were started at 6 months of age (25). These results were also replicated in mice, with their resting temperature dropping by 13^{o} C (24). The body

temperature in rats was also shown to drop due to CR, but only by 2^{o} C (26). This indicates that CR decreased oxygen consumption and subsequently reduced oxidative damage (28).

There is also evidence that metformin's CR mimicking action can mediate the reduction of harmful oxidants in humans. The generalized action of CR has been found to be responsible for reducing oxidative damage in the body, increasing maximal life span and indicating overall anti-aging benefits (27).

For example, one study by Rabbani *et al*. examined how metformin affects oxidative damage in apolipoprotein B100 of LDL particles in blood (28). High levels of LDL particles in blood are a strong indicator of type 2 diabetes-related cardiovascular disease as it indicates ineffectual LDL clearance from LDL receptors and hepatic over-secretion of apolipoprotein B100 (28). Along with oxidation of apolipoprotein B100, protein glycosylation and nitration also contribute to high LDL particles levels (28). Venous plasma LDL composition from type 2 diabetics and healthy control patients was analyzed through stable isotopic dilution analysis tandem mass spectrometry (28). The results indicated that metformin decreased the amount of arginine-derived advanced glycation end products and oxidative damage in apolipoprotein B100 of LDL (28).

In addition to its role in reducing oxidative stress-related CR in type 2 diabetes, metformin also reduces oxidation of other biomolecules. For example, another study by Algire *et al*. (29) elucidated the beneficial effects metformin can have on DNA damage caused by oxidative stress. The study looked at reactive oxygen species (ROS) related to DNA damage and mutations. Several $AMPK^{+/+}$ and $AMPK^{-/-}$ mouse embryonic fibroblast (MEF) cell cultures were created and exposed to varying conditions that typically increase the amount of ROS. Metformin reduced paraquat-induced, but not H_2O_2-induced, elevations of ROS in an AMPK-independent

manner (29). This indicated metformin's effectiveness in reducing endogenous ROS production (29). In paraquat-exposed cells, metformin reduced DNA double strand breaks and somatic cell mutation rates while also improving mouse survival (29).

Multiple studies have looked at metformin's ability to treat neurological ailments and ameliorate oxidative damage located in the brain and collectively suggest an extension of neural longevity. There are multiple benefits to metformin-mediated amelioration of neural oxidative stress including preventing apoptotic cell death, memory impairment, cerebral ischemia and epileptic seizures (30, 32, 33, 34). A study by Zhao *et al*. (30) on male C57BL/6 mice found that metformin treatments were able to mitigate neural oxidative stress and cognitive impairment associated with seizures and epilepsy. Another study by El-Mir *et al*. (31) examined diabetes-related neuronal disorders and the effect metformin treatments might have on longevity found that oxidative stress can increase instances of etoposide-induced cell death on primary cortical neurons taken from rats.

Through further exploration of this topic by researchers, more effective metformin-based treatments can possibly be developed to produce more optimal patient outcomes. Collectively, the majority of research findings indicate the effectiveness of metformin treatment in type 2 diabetics to reduce the overall aging effects due to oxidative damage (29).

1.8 Effects on telomere length

Telomere length is another model of aging that is becoming more frequently used to measure longevity. Telomeres are specific sequences of non-coding DNA that 'cap' the coding region of linear chromosomes, protecting it from degradation or enzymatic modification through

nucleolytic resection or fusion (35, 36). Structurally, telomeres are nucleoprotein complexes that include guanidine-rich repeated sequences within the DNA (36). The repeat sequence is the hexamer TTAGGG (35, 83).

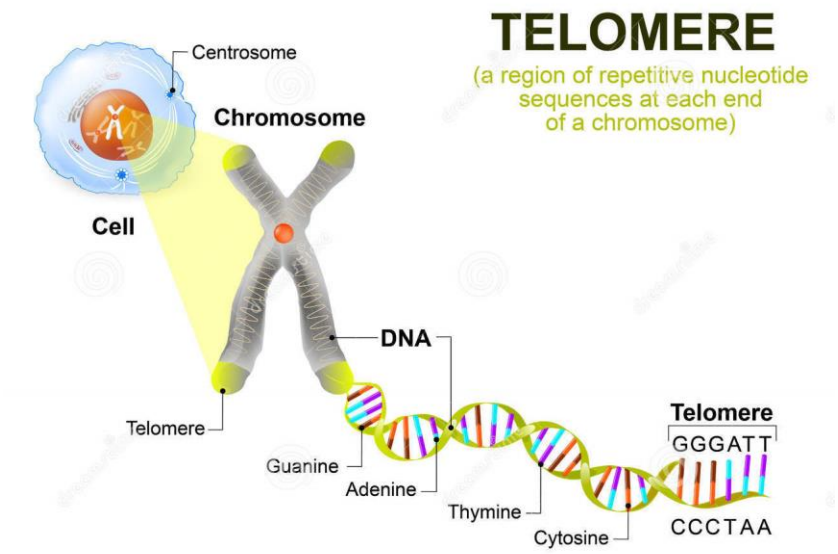

Figure 4: Location and structure of the telomere on a human chromosome (83).

Telomeres have been shown to shorten with each cell division for many human tissues, disappearing completely after enough successive divisions (37). This is caused by a phenomenon known as the 'end-replication problem', in which, due to the unidirectional 5'→3' synthesis of DNA, some bases on the 3' end remain uncopied after replication in the S phase (39). In the absence of telomeres, the DNA sequence can undergo degradation and the chromosome ends can become fused and destabilized. As a consequence, the cell will no longer be able to replicate, and enters a state of senescence in which the cell will cease to divide further (37).

Limits to human cell division were first observed by Leonard Hayflick (35) who experimented with human tissue cells that were repeatedly cultured. Although Hayflick was able

to categorize the type of growth that occurred into three phases, with "Phase 3" displaying senescence, it was unknown at the time what caused this outcome (36). Senescence has since been shown to have many possible causes, many of which are environmental stresses (36). However, even in a stress-free environment, senescence is still inevitable (36). An accumulation of senescent cells in human tissue can result in the expression of the senescence-associated secretory phenotype (SASP) (119). Cellular senescence caused by a SASP has been shown to produce pro-inflammatory cytokines, chemokines, growth factors and proteases, leading to a damage in tissue structure and function that is characteristic of aging (119).

The phenomenon of cellular senescence was first posited to be attributed to the gradual loss of telomeric DNA in the cells by Olovnikov in 1973 (122, 123). In 1992, Harley et al. built upon this concept, proposing that telomere length is shortened to a predetermined size in where a "genetic check-point" is reached, and the Hayflick limit is consequently initiated, halting cellular division (123). This phenomenon of progressive shortening with age was observed both in vivo and in vitro for somatic cells by Harley et al (123, 124). Gametes, such as sperm cells, do not display this, and their telomeres remain long without decreasing with age (123). This retention of telomere length is due to the presence of telomerase, which is active predominantly during gametogenesis (120, 123)

Telomerase is a guanidine-rich ribonucleoprotein enzyme that can be used to synthesize the repeated TTAGGG/CCCTAA sequences of which telomeres comprise (38, 45). Telomerase acts similarly to a reverse transcriptase, and it is essential for complete replication of telomeres within DNA. It should be noted that, in humans, most somatic cells, such as fibroblasts, epithelial cells, melanocytes, endothelial cells, and astrocytes, do not express the telomerase enzyme and will thus eventually senesce (119, 45, 121).

Because of telomerase's inactivation in somatic cell replication, as well as its noted activity in cancer cells, several studies developed ways to better understand the nature of this enzyme (18, 80, 120, 125, 126). Five independent research groups were able to concurrently clone human telomerase reverse transcriptase (hTERT), a subunit of telomerase (18, 80, 120, 125, 126). Through the examination of hTERT reactivation, these studies were able to conclude that hTERT functions as the catalytic domain of telomerase and its expression is essential for the telomerase-mediate reverse transcription of human telomeres (18, 80, 120, 125, 126).

In 1998, the researchers from the Geron Corperation were able to establish a causal relationship between the process of telomere shortening and in vitro cellular senescence (45). They demonstrated telomerase's ability to extend the replicative ability of normal human somatic cells while maintaining their diploid status, growth characteristics, and expected gene expression pattern (45). Another study from the same year, by Vaziri and Benchimol, demonstrated similar findings, showing how the rejuvenation of telomerase activity in vivo was able to extend cellular life span through the increase in telomere length (19).

Due to the natural shortening of telomeres in somatic cell with each cellular division, it can be logically assumed that there is a correlation between telomere length and aging. Many studies have confirmed this assumption, demonstrating strong correlations (40) (Figure 5). Therefore, telomere length could be used as effective biomarker for aging (41).

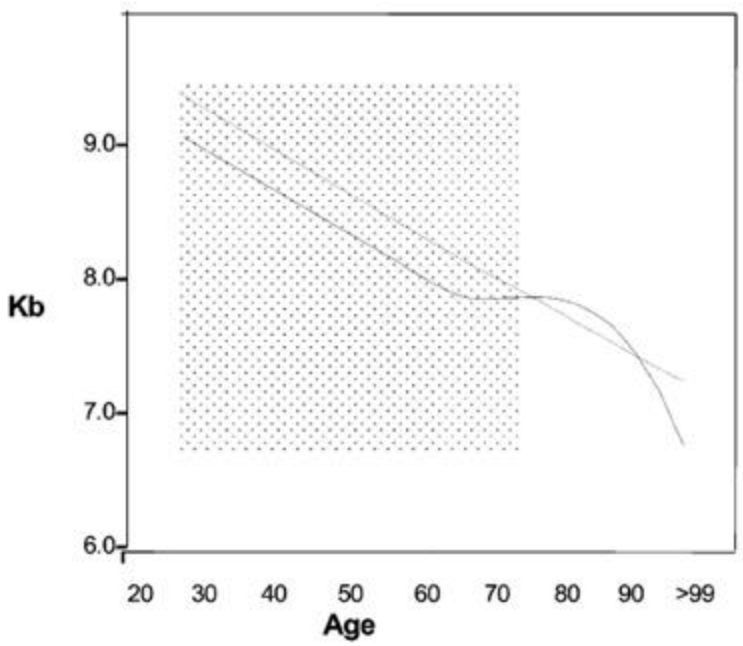

Figure 5: The rate of telomere shortening from early adulthood to old age using DNA samples extracted from whole blood (77).

One preclinical study took a multimodal approach to examine metformin's effects on longevity in prediabetic patients by examining several aging-related parameters (42). Gene transcription levels and protein levels of mTOR, p53, p66Shc, and sirtuin-1 (SIRT1) were examined in both individuals taking metformin and those assigned a placebo (42). SIRT1 activity as well as AMPK activation, telomere length, peripheral blood mononuclear cell (PBMC) levels and N-glycan levels were also studied in both individuals taking metformin and those assigned a placebo (42). Out of 38 prediabetic patients, 19 were assigned to take 3x500 mg metformin tablets daily for two months, while the remaining 19 received the placebo treatment (42). The results found that some effectors of longevity pathways were modified (43). Metformin was found to moderately increase SIRT1 expression, reduce p70S6K phosphorylation, and favorably modified the plasma N-glycan profile (42). Telomere lengths of PBMCs were found to have increased significantly from the baseline levels after metformin treatments and did not increase

with placebo treatments (42). However the degree of change from the baseline for both groups was not significantly different from each other (42).

The effect of metformin on reducing disease risk can be difficult to determine due to the complex etiology of many age-related human diseases. One study looked at potential links between type 2 diabetes, oxidative damage and colorectal carcinoma by measuring telomere length (43). While some of the study participants were taking metformin treatments, the efficacy of the drug was not tested (43). In addition to those participants undergoing treatments of metformin alone, others were prescribed treatments of sulfonylureas, both metformin and sulfonylureas in combination, and subcutaneous insulin (43). Overall, results indicated that mean colonic epithelial telomere length in participants with type 2 diabetes was not significantly different from the control values (43). Therefore, no link was found between telomere shortening due to type 2 diabetes and colorectal carcinoma.

Further colorectal cancer research examined how metformin affects telomeres in human colon carcinoma cells by studying the drug's effects on the proliferation of SW-480 cells (44). Telomerase activity was examined through telomeric repeat amplification protocol (TRAP) silver staining (44). It was found that metformin treatments were able to decrease telomerase activity, inhibiting the growth of SW-480 cells (44).

Endometrial cancer cell proliferation was also examined in a study by Cantrell et al. (46) which investigated the effects metformin treatments had on human telomerase reverse transcriptase (hTERT) activity. The hTERT is an essential catalytic subunit of telomerase which is a guanidine-rich ribonucleoprotein enzyme that can be used to synthesize the TTAGGG/CCCTAA sequences in human telomeres (38, 45). Telomerase acts similarly to a reverse transcriptase, and it is essential for complete replication of telomeres, eliminating the

end-replication problem that would normally degrade the entire telomere sequence over time (45). qPCR was used on endometrial cell lines to measure hTERT gene expression (46). It was found that, within 24 hours of treatment with metformin, hTERT mRNA expression was decreased (46). As hTERT expression is considered a rate-limiting step in the production of telomerase and telomerase is needed for telomere extension, it appears that, in endometrial cells, metformin treatments will reduce telomere length. A reduction in telomere length could indicate a decrease in longevity for this particular cell type. Hanna and Zhou (47) further built upon this research to find that a combination treatment of metformin and paclitaxel may be more effective at maintaining telomere length. This potentiating effect seems to derive from metformin's ability to inhibit cell proliferation while simultaneously modulating the mTOR pathway (47).

1.8.1 Health conditions related to telomere length

Damage to the chromosomal sequence can lead to many adverse health outcomes as well as increased mortality. Shortening of telomeres has been linked to atherosclerosis, dementia, post-stroke mortality, cognitive decline, diabetes, and cardiovascular disease (40, 86, 87, 88). Prevalence for these pathologies has been shown to increase as the telomere length decrease (40, 86, 87, 88).

The opposite is found in studies looking at telomere shortening and cancer. Many types of cancer have been found to increase in prevalence with longer telomere lengths. Telomerase has been shown to be active in tumorous tissues, leading to the prevention of telomere shortening (89). This immortalization of tissue results in oncogenesis and out of control cell growth (89).

1.8.2 Lifestyle factors related to telomere length

There are also several lifestyle factors that have been shown to correlate with telomere length. Oxidative stress has been shown to increase the rate of telomere shortening and the characteristic cellular senescence (90). Antioxidants will work contrary to this type of shortening, preventing telomere shortening (90). Life stressors, dietary differences, or childhood trauma have also been shown to correlate with telomere shortening (91, 92).

1.8.3 Demographic factors related to telomere length

Demographic factors such as gender and biogeographic ancestry also correlate with telomere length (14). Males, on average, have shorter telomeres than females and Caucasians, on average, have shorter telomeres than other biogeographical groups (40).

1.9 Methods of measuring telomere length

There is currently a diverse array of techniques that are being utilized to a high degree of effectiveness to measure telomere length. Southern blotting methods, widely considered to be the 'gold standard' technique for telomere length measurement, are but one way to accurately measure telomere length (93, 94). Quantitative PCR, quantitative fluorescence in-situ hybridization (q-FISH), Single Telomere length analysis (STELA) and other methods are also effective, each having their own unique set of advantages and limitations (93, 94).

The Southern blot technique for measuring telomere length was originally developed by Kimura *et al*. (94) for examining leukocyte telomere length (LTL) in epidemiological studies. The procedure begins with genomic digestion with a 'cocktail' of frequent cutting restriction enzymes (lacking telomeric and subtelomeric recognition sites) (94). The technique then makes

use of gel electrophoresis, followed by labeled probe hybridization for telomere sequencing (95). The different telomere lengths will be visualized through gel imaging, presenting as a smear to which the size and intensity can being assessed via comparison to a DNA ladder (93, 96). This method is also known as terminal restriction fragmentation, with the unit of measurement for the telomere length being telomere restriction fragments (TRFs) (94).

Due to the frequency of use of the Southern Blot technique, the majority of literature contains the length of TRFs, allowing for more opportunities of direct comparison to occur (94). This method is also relatively cheap, with high reproducibility (93, 94). It also allows for the possible determination of telomere length distribution, however this is rarely completed in epidemiological studies due to difficulty in obtaining accurate gel measurements (93). One disadvantage is that the Southern blot method generally requires a substantial amount of DNA (3 μg per sample) (93). It also requires the measurement of both the telomeric and sub-telomeric regions (93). Problems can also arise if the sub-telomeric regions lead to artificial inflation (93). There can also be variations in the TRF values if a different cocktail of restriction enzymes is used (97).

Quantitative PCR is another method that is becoming more and more prevalent in the measurement of telomeres. Richard M. Cawthon (97) was the first to propose a method of measuring telomere length via qPCR. This method analyzes the relative telomere length per DNA sample (97). It compares the factor by which the sample differed from reference DNA and its ratio of telomere repeat copy number to single gene copy number (97). The ratio used is proportional to the average telomere length (97). Two serial dilutions are made with reference DNA (97). One serial dilution is completed with amplifications of the telomere repeat sequence for the reference DNA sample, and the other is completed with the amplification of a single copy

gene for the reference DNA sample (97). Once they have been amplified through the Real Time PCR thermocycler, the resultant Cq (equivalent to Ct, or cycle threshold) values for the serial dilutions can be plotted against the logarithmic values of their corresponding copy numbers in a standard curve. The tested sample can be compared to both serial dilutions to find the telomere repeat copy number and single gene copy number respectively (97). Relative telomere length is obtained by dividing the telomere copy number by the single gene copy number (T/S) (97). Cawthon's qPCR method can produce results from more minute quantities of the initial sample than the Southern blot method (97). It also has the benefit of being able to provide a high-throughput performance (93, 35).

The Cawthon method was modified by Nathan J O'Callaghan and Michael Fenech to include an oligomer standard, allowing for the measurement of absolute telomere length instead of relative telomere length (35, 98). Absolute telomere length can be a direct comparison of results between other experimental values from other labs (35).

In general, qPCR is able to produce results from more minute quantities of initial sample than the Southern Blot method because of this, buccal sampling, or any other low-quantity sampling, would be compatible with this methodology (93, 97). It also has the benefit of being able to provide a high-throughput performance, increasing the ease, amenability and speed of the analysis (93, 94, 35). One limitation of qPCR telomere analysis is that it has a high variance of between 5 and 10%, making it more difficult to notice differences between samples and control (93). Like the Southern blot techniques, qPCR-based techniques require high-quality, non-compromised DNA samples (94). Also, the choice of the reference gene used can cause variance in the data due to differences in stability (93). Reference genes, such as 36B4, albumin and β-globin, are common, yet there is no standard gene that is universally used (93).

The Southern blot and qPCR methods are also limited in that they can only determine the average telomere length of the specimen being evaluated, and do not provide information that specifically applies to the individual telomere lengths within a chromosome (94). The STELA method is a unique telomere measuring technique that does allow for the analysis of a single chromosome (37). This ligation-based method, originally developed by Baird *et al*. (37), targets the amplification of the telomeric portion of a single chromosomal end, by using primers that bind to the specific sub-telomeric sequences of a single chromosome. This procedure is only valid for measuring a small subset of chromosomes (Xp, Yp, 2p, 11q, 12q and 17p) (99). Also, differences in the rate at which specific telomeres shorten might render this technique ineffective in recognizing critically short telomeres (100).

A modified method, referred to as the universal STELA technique, solves this problem by allowing any critically short telomere to be detected regardless of its location on the chromosome (100). This method involves three main steps digestion, ligation and amplification (100). The DNA of interest is first digested by a selection of restriction endonucleases, and then a ligation step allows for the suppression of the amplification of the intra-genomic fragment (100). Lastly, the samples are sequentially ligated and then amplified for the short telomeric regions (100).

Both the original and modified STELA methods are able to detect telomeres in a single chromosome from very low-quantity samples (94). However, both methods are limited in that they are unable to measure telomeres having long lengths (over 8kb) (100). This could mean that these methods might be misleading in samples from cancer cells or from very young individuals (101, 89).

Fluorescence in situ hybridization (FISH) has frequently been incorporated in many methods that measure telomere length. Quantitative fluorescence in situ hybridization is one of these methods, measuring the length of the telomeric repeats (94). It was first developed Peter Lansdorp and colleagues and, shortly after, adapted by Krejci and Koch (102, 103). The q-FISH method differs from TRF and PCR-based assays by using cells as the substrate rather than the DNA itself (94). This method is accomplished by assessing the metaphase chromosomes or interphase nuclei following fluorescent labeling with a $(CCCTAA)^3$ probe (94). Any remaining chromatin on the chromosome is visualized by a nonspecific DNA stain (such as 4',6-diamidino-2-phenylindole [DAPI] or propidiumiodide (102). The probe typically chosen for the assay is a synthetic peptide nucleic acid (PNA) probe (94). This is because the probe has a neutral backbone, causing it to produce more efficient hybridization than DNA probes (104). The q-FISH method is able to estimate the size of each of the 92 telomeres and it is not limited to measuring average or small-size telomeres (94). Another benefit is that this method can also recognize the ends of a chromosome that would typically be too small to adequately hybridize (94). The q-FISH method has been optimized for a variety of conditions and samples for biological testing (106). It has also been shown to be useful for measuring the telomere length in rare cells such as $CD34^+$ cells in bone marrow from individuals suffering from dyskeratosis congenita (105). The main weakness of the metaphase q-FISH technique is its inability to measure telomeres in cells that are not actively undergoing mitosis (such as terminally senescent cells) (94). Its functionality is also limited in specimens with very slow proliferation rates (94).

There are two main categories of q-FISH: metaphase q-FISH and interphase q-FISH (94). Metaphase q-FISH studies are useful for obtaining information about differences in telomere length between different chromosomes, and also for providing information about the frequency

of chromosomal instability associated with chromosomes with very short unhybridizable telomeres (107). This form of q-FISH is not suitable for large epidemiological studies due to it being labor intensive, expensive, and technically demanding (requiring experience with chromosomal banding patterns) (94).

Interphase q-FISH was developed to overcome some of these limitations associated with metaphase q-FISH (94) utilizing interphase cells and its chromosomes rather than metaphase chromosomes. Interphase q-FISH is also able to assess telomere lengths in nuclei from a variety of different specimen types (94). Often in interphase q-FISH, a fluorescent signal obtained from a telomere-specific probe is compared to a centromeric probe or a differing coloured fluorophore (94). Next a ratio of signal intensity between the targeted sequences can be calculated (107). Interphase q-FISH is beneficial in telomere length analysis because it allows for the concurrent collection of information regarding telomere length and information about the tissue sample (94). It is also less labor intensive than metaphase q-FISH (94). This information can be used alongside immunostaining techniques to localize specific cells of interest in a process that is sometimes referred to as telomapping (108). A limitation of the interphase q-FISH technique is that it does not allow for the recognition of specific telomeres, or for the detection of chromosomal ends with very short unhybridizable telomeres (94). Also, the data is usually measurable in terms of a mean value for all 92 telomeres (94) and can be automated in a form known specifically as high throughput q-FISH (HT q-FISH) (101). This method was developed to maintain accuracy and improve efficiency in q-FISH, allowing for these methods to be used in larger epidemiological studies (93, 94, 101). The HT q-FISH method can also improve the efficiency of flow cytometry plus traditional FISH techniques (93).

Another method, flow cytometry plus FISH technique, was developed by Baerlocher *et al*. (109), in order to measure the mean telomere length with metaphase staining. Flow-FISH methodology also utilizes the $(CCCTAA)^3$ PNA probe for quantification of the mean amount of fluorescence in the cells, and the average telomere length for that cellular population (110). This method could be used to measure from any subpopulation of circulating peripheral cells due to the initial flow cytometry step (109). Consequently, flow cytometry plus FISH was able to determine the telomere length for individual cells of a distinct cell type and the distribution of telomere lengths of that cell type (93). Furthermore, this method utilizes an internal reference control and highly specific nucleic acid probes to hybridize to the telomeric repeats, greatly improving the accuracy (93). Flow cytometry plus q-FISH is the first of the telomere assays to be used as a clinical diagnostic tool, assisting with the recognition of congenital dyskeratosis (111). This method can also allow for the inference of a three-dimensional distribution of telomeric signals in cells (112). Despite providing more information than other methods, flow cytometry plus FISH is quite expensive, highly inefficient, and requires a high degree of technical expertise that could limit its use in epidemiologic research (93).

The primed *in situ* (PRINS) method of measuring telomeres utilizes fluorescently tagged nucleotides and PCR techniques with telomeric primers which label the telomeric sequences *in situ* on metaphase chromosomes or interphase nuclei (113). This method is used in lieu of a PNA probe to label the telomeres in preparation for analysis using q-FISH methods (113). Therefore, the sample benefits and limitations of that method apply to PRINS techniques (93).

The hybridization protection assay (HPA) involves the comparison of telomeric to *Alu* repeats present in a specimen (114). This method was designed to be faster and easier to read than the traditional Southern blot technique, improving the overall accuracy of the results (114).

This method involves adding the sample to a hybridization solution containing acridinium ester-labeled probe, followed by a differential hydrolyzation with the unhybridized probe. The chemiluminescence results are then measured through imaging (114). Along with its speed (around 45 minutes), this technique does not require high quality DNA, or even large quantities (94). However, one limitation is that it is difficult to interpret the ratio values due to variation in the *Alu* repeat sequences between samples (93). Only a mean value of telomere length, with no cell- or chromosome-specific data is generated (93).

Alternate methods also exist which quantify the length of the telomeric 3'overhang instead of the full telomeric length. Some techniques that follow this approach include telomereoligo (oligoneucleotide) length assistance (T-OLA), G-tail HPA, overhang protection assay (OPA), single-strand electron microscopy, primer-extension nick translation (PENT) and double-strand specific nuclease (94, 115, 116, 117, 118). These techniques have important biological applications and usually produce more focused outcomes (94).

After considering the limitations and advantages of the telomere measurement methods above, as well as the equipment available in our lab, we chose to use qPCR in our study. Prior professional experience and success with this method as well as low processing time were deciding factors for choosing this method. Additionally, the relatively low cost of qPCR analysis allowed for this project to be economically feasible.

1.10 Summary and future prospects

Currently, there are many studies examining the benefits of metformin treatment when prescribed for both its approved treatment of type 2 diabetes and off-label as a geroprotectant. Currently, more and more evidence supports the notion that metformin has geroprotective properties. With further information about the exact nature of metformin's effects, and deeper

insight into its various interactions with biochemical pathways in the human body, therapeutic treatments can possibly be further developed.

Prior to its approval as a geroprotectant, more research should be done on metformin's effectiveness on preserving telomere length. Although studies have found that metformin can increase the length of telomeres and delay shortening, further human studies are needed because evidence indicates that metformin use may be more beneficial with more prolonged treatments. It would be valuable to have clinical trials that measure possible benefits of long-lasting metformin therapies. Future studies examining the specific benefits of the drug at all stages of life would also be useful. As well as subcategorizing subjects by age cohorts, it would also be useful to separate data based on biological sex due to the noted differences in health outcomes between men and women. Standardization of telomere length measurement methods is also needed to more easily compare treatment effects between studies, so that telomere measurements and general patterns and revelations from these prospective metformin studies can be replicated via differing telomere-measuring methods such as the Southern blot method, STELA or the q-FISH.

With additional examination into this relatively novel area of research, further understanding of the effects metformin has on aging and longevity can be determined, with the potential for more refined and effective metformin therapies being developed as a result.

2: Materials and methods

2.1 Ethics approval and sample collection

All protocols were approved by the Lakehead University Research Ethics Board (Project #067 16-17). Primary patient recruitment was through the Curans Heart Centre, an outpatient cardiac clinic located in Thunder Bay, Ontario. Patients were recruited either through posters and pamphlets advertising the study or directly, where individuals taking metformin and/or who have type 2 diabetes, were informed about the study by their nurse practitioners and asked if they would be interested in participating in the study. All participants' results of their telomere analysis (once the research has been published) along with a contextual comparison to the population average for their age cohort were emailed to each participant.

All participants were required to complete a consent form which included a brief questionnaire and a space to provide their email should they desire access to the results. The questionnaire asked the participant's age, biological sex, whether they had type 2 diabetes, and if they were currently taking metformin. Once the consent form was completed, the nurse practitioner collected it and inputted the answers to the questionnaire and the patient's personal information into a Microsoft Excel spreadsheet that was saved to a secure server. Each participant's sample was assigned a random sample number and this number was recorded on the Excel spreadsheet along with their information. The Excel spreadsheet was only provided to the researcher once the data had been collected, analyzed, and tabulated for each random sample number, allowing the study to remain blind. Once all the information has been collected, the nurse practitioner took the blood with a 22 gauge needle and a 5 mL syringe. The blood was then deposited into a 3 mL Greiner Bio-One Hematology K_3 EDTA Evacuated Tube.

2.2 Sample storage

Blood samples were stored in a 2° C fridge temporarily (1-7 days). The samples were collected weekly from Curans Heart Centre and brought to the laboratory at Lakehead University. There, the samples were centrifuged at 13,000 rpm for 10 minutes. Afterward, the blood in the sample tube was separated into three components: the red blood cells at the bottom, the buffy layer containing the white blood cells in the center and the plasma at the top. An aliquot, 200 μL of the central buffy layer was removed via a micropipette and deposited into a 2 mL microcentrifuge tube and labeled with the sample number. All lab work was conducted in a biosafety cabinet. All purified sample DNA solutions were stored in a -20° C freezer for up to 2 months.

2.3 DNA extraction and purification

All DNA from the blood samples was extracted and purified using the Invitrogen PureLink Genomic DNA Mini Kit. All procedures followed the steps outlined in the PureLink Genomic DNA Kit user manual on pages 17, 23 and 24, which outline the protocol for a blood lysate DNA extraction and purification (76). In part 2 of the blood lysate extraction protocol (page 17), a suggested alternative to the default extraction procedure was implemented with 100 μL of the blood lysate sample used alongside 100 μL of phosphate buffered saline (PBS) (76). During the 'Eluting DNA' step (page 24), 75 μL of the Genomic Elution Buffer was added to the washed DNA spin columns to produce purified DNA of a moderate concentration (as outlined on page 13). The newly purified DNA samples were stored in a -20° C freezer for up to 1 month.

2.4 DNA quantification

Dyed master-mix solutions consisting of 198 µL of Tris-EDTA (TE) buffer, 0.5 µL QuantiFluor dsDNA dye and 2 µL of the purified sample were made and vortexed thoroughly. All samples were then quantified with a Promega Quantus fluorometer in triplicate. The concentration of the DNA solution was displayed through the Quantus software installed on an HP laptop computer. Data was then exported to Microsoft Excel, and the average concentration for each purified sample was determined. Quantifications of the telomere and 36B4 standards were also completed and would be necessary for the qPCR calculations in part 2.5.

2.5 Preparation of samples, standards and primers for qPCR

Using the average concentration of each purified sample, the amount of double distilled water (ddH_2O) required to dilute the sample to a concentration of 5 ng/µL was calculated (see Appendix A) (35). A 100 µM stock solution was created for both standards and both sets of primers (see Appendix B). Primers were further diluted with ddH_2O by a factor of 10 into 1/10 working primer solutions. Standards were also diluted with ddH_2O into serial dilutions. Two sets of standards were created: a synthetic telomere standard to serve as a positive control reference for the amount of telomere hexomeric repeat sequences amplified per sample and a 36B4 standard which encodes for the acidic ribosomal phosphoprotein P0 that serves as a positive control for the number of single gene copies (SCGs) amplified per sample (35). Both standards had 10^5, 10^6, and 10^7 serial dilutions included in each qPCR run. Based on the DNA concentrations quantified in part 2.4 by the Quantus fluorometer, the number of telomeres and SGCs were calculated for the telomere and the 36B4 standards respectively. These calculations

were completed according to O'Callaghan *et al*. (35) and the calculation steps can be seen in Appendix A.

2.6 qPCR

All PCR runs were completed by first creating two qPCR master mixes (one for each primer set), which both consisted of 10 µL of PerfeCTa SYBR Green Supermix, 1 µL of the forward primer, 1 µL reverse primer, and 4 µL ddH_2O (35). Each qPCR reaction had a master mix total volume of 16 µL added to 4 µL of the DNA sample (at a concentration of 5 ng/µL) (35). The qPCR master mix solution was added to each well of a 96 well PCR plate. Each sample, as well as the serial dilutions for both standards, were then added, in triplicate, to the master mix solution in each well.

Once all the samples were added, the plate was then sealed and placed inside a Bio-Rad CFX96 Optics Module Real Time System C1000 Thermocycler. The thermocycler was set using the Bio-Rad CFX manager software. The cycling conditions were set to be 10 minutes at 95° C, followed by 40 cycles of 95° C for 15 seconds, 60° C for 1 minute, followed by a dissociation (or melt) curve. Once the qPCR was completed, the data were exported to a USB memory device and examined later with Microsoft Excel.

2.7 Data analysis

The results were analyzed using the Biorad CFX manager software and Microsoft Excel. The amplification curves were analyzed, and non-sigmoidal curves excluded from analysis. The Cq values were plotted against the known telomere quantities (in units of kb) and the SGC

numbers for both the telomere and 36B4 standard curve respectively. The Cq values from the samples amplified with the telomere primers were then compared to the telomere standard curve to elucidate the quantity of telomeres (in units of kb). All Cq readings were completed in triplicate and were averaged.

Any outlier Cq values were eliminated before analysing the results. First the appearance of the amplification curves for each triplicated amplification runs was visually compared with one another. If one of the three curves appeared markedly shorter or steeper than the other two, with more than a 25% difference in height, the Cq value corresponding to that curve was eliminated. If any curve did not display the characteristic sigmoidal shape of a logarithmic amplification, it would be eliminated as well. All triplicated Cq values were also examined based on their numerical values. If a Cq value was markedly different than the other 2, with a percent difference of 25% or greater, it would be eliminated. If all Cq values were reasonably evenly dispersed, then all three values would have been calculated to determine the average

The Cq values from the samples amplified with the 36B4 primers were also compared to the 36B4 standard curve to find the number of SGCs. The absolute telomere length per genome was determined by dividing the quantity of telomere by the SGC number. This number was further divided by 46 to determine the average absolute telomere length per chromosome. These calculations and a data sample are shown in Appendix C.

Data was arranged into one of four possible cohort groups: Samples from non-type 2 diabetic who did not take metformin (referred to as Cohort 1), samples from type 2 diabetics who did take metformin (referred to as Cohort 2), samples from type 2 diabetics who did not take metformin (referred to as Cohort 3), and samples from non-type 2 diabetics who did take metformin (referred to as Cohort 4). When analyzed, cohorts were not further subdivided into

ethnic origin, education, health/activity, or socio-economic status due to the limitations of the sample size. No information was taken about the dosage of the metformin or the treatment duration.

The data was truncated to only include average absolute telomere lengths from samples of individuals 41 and older. This was because the data from participants under the age range of 41-50 was homogenous, all belonging to Cohort 1. This information has limited use as it cannot be compared to other cohort groups within similar age ranges. Truncation of this data is useful as it allows the cohort groups to be more accurately compared and reduces the potential for the Cohort 1 data to be skewed due to having a large amount of younger samples.

The final average absolute telomere length values were determined to be outliers if they were over 15 kb/chromosome or less than 0.1 kb/chromosome. Since it has been demonstrated through the literature that newborn telomere lengths typically fall between 15 and 20 kb/chromosome, final average absolute telomere lengths over 15 kb/chromosome were considered to be outliers and were not included in the final analysis (78). Similarly, since average absolute telomere lengths under 0.1 kb/chromosome can be approximated to zero, any values below this threshold were also deigned to be outliers and were eliminated as well.

2.8 Statistical analysis

Regression analysis was first completed for all cohorts using IBM SPSS Statistics Data Editor. Next, t-tests were completed in Microsoft Excel 2016, which compared the data of Cohort 1 and Cohort 2, Cohort 1 and Cohort 3, and Cohort 2 and Cohort 3. Lastly, GraphPad Prism 7.05 was used to generate a one-way ANOVA test which compared Cohorts 1, Cohort 2, and Cohort 3.

3: Results

The four cohort groups are referenced as such: Cohort 1, Cohort 2, Cohort 3, and Cohort 4. Cohort 1 contains participants equating to the non-type II diabetic and non-metformin samples, Cohort 2 equating to the type II diabetic and metformin samples, Cohort 3 equating to the type II diabetic and non-metformin samples, and Cohort 4 equating to the non-type II diabetic and metformin samples.

3.1: Telomere length measurements

Telomere length is provided in two forms for all samples: absolute telomere length per genome and average absolute telomere length per chromosome this allows for a more direct comparison to literature values. These measurements will be presented as mean values in units of mean average absolute. The telomere lengths were calculated (see example in Appendix A) and a compilation of all telomere length data obtained from separate qPCR amplifications (Table 1). Relevant, anonymized participant information is also presented here for direct comparison. The sex, age, diabetic status, and metformin use were all obtained from Curans Heart Centre and provided to the researchers after final calculations of telomere length. Samples from individuals over the age of 41 years were included in the analysis and interpretation. However all data is included here to provide a comprehensive list and support the validation of the qPCR results.

Table 1: A compilation of all quantified telomere lengths for the anonymized samples that were analyzed through qPCR amplification.

Participant Number:	Sex:	Age:	Diabetic Status:	Metformin Use:	Absolute telomere Length per genome (kb)	Average absolute Telomere length per chromosome (kb)	Cohort Group:
87	F	19	Non-Diabetic	No	219.7747297	4.777711515	Cohort 1
89	M	19	Non-Diabetic	No	174.7469764	3.798847312	Cohort 1
91	F	19	Non-Diabetic	No	173.8538493	3.779431506	Cohort 1
76	M	20	Non-Diabetic	No	31.3279346	0.681042056	Cohort 1
77	M	20	Non-Diabetic	No	185.2797512	4.027820677	Cohort 1
88	F	20	Non-Diabetic	No	111.8700451	2.431957502	Cohort 1
172	F	20	non-Diabetic	No	13.41411709	0.291611241	Cohort 1
10	F	21	Non-Diabetic	No	870.5679517	18.92539025	Cohort 1
15	M	22	Non-Diabetic	No	182.5106574	3.967622986	Cohort 1
155	F	23	non-Diabetic	No	19.97200011	0.434173915	Cohort 1
169	F	23	non-Diabetic	No	162.3344055	3.529008815	Cohort 1
84	M	24	Non-Diabetic	No	182.4098576	3.965431686	Cohort 1
175	M	24	non-Diabetic	No	278.334279	6.050745195	Cohort 1
1	F	25	Non-Diabetic	No	128.6298684	2.796301487	Cohort 1
92	F	25	Non-Diabetic	No	343.9382361	7.476918176	Cohort 1
161	F	25	non-Diabetic	No	328.4164295	7.139487599	Cohort 1
7	F	26	Non-Diabetic	No	208.2728414	4.527670466	Cohort 1
160	M	26	non-Diabetic	No	97.95116803	2.129373218	Cohort 1
162	F	26	non-Diabetic	No	286.0970147	6.21950032	Cohort 1
40	F	27	Non-Diabetic	No	443.2590608	9.636066539	Cohort 1
115	F	27	Non-Diabetic	No	48.17006445	1.047175314	Cohort 1
23	F	28	Non-Diabetic	No	68.17244989	1.48200978	Cohort 1
156	M	28	non-Diabetic	No	75.62698996	1.644064999	Cohort 1
157	F	28	non-Diabetic	No	3.157556279	0.068642528	Cohort 1
159	M	28	non-Diabetic	No	154.4473124	3.357550271	Cohort 1
170	M	28	non-Diabetic	No	36.08898464	0.784543144	Cohort 1
176	M	29	non-Diabetic	No	1637.260978	35.59262996	Cohort 1
14	F	30	Non-Diabetic	No	248.1199084	5.393911051	Cohort 1
2	F	35	Non-Diabetic	No	3.191125551	0.069372295	Cohort 1
13	M	35	Non-Diabetic	No	160.8193517	3.496072864	Cohort 1
8	F	36	Non-Diabetic	No	4.660159858	0.101307823	Cohort 1
9	M	39	Non-Diabetic	No	0.377880114	0.008214785	Cohort 1
42	F	39	Non-Diabetic	No	67.3373124	1.463854617	Cohort 1
22	F	42	Non-Diabetic	No	153.324347	3.333137979	Cohort 1
151	M	42	Type 2 Diabetes	Yes	183.5970094	3.991239336	Cohort 2
167	F	45	non-Diabetic	No	26.84531477	0.583593799	Cohort 1

28	F	46	Non-Diabetic	No	44.1599349	0.959998585	Cohort 1
82	M	46	Non-Diabetic	No	66.80082356	1.452191816	Cohort 1
74	F	47	Non-Diabetic	No	539.9246413	11.7374922	Cohort 1
120	M	47	Type 2 Diabetes	Yes	95.12266713	2.067884068	Cohort 2
12	F	48	Non-Diabetic	No	115.8060353	2.517522507	Cohort 1
27	F	49	Non-Diabetic	No	363.5195346	7.902598578	Cohort 1
93	M	50	Non-Diabetic	Yes	36.51424011	0.793787829	Cohort 4
83	F	50	Non-Diabetic	No	191.5011221	4.163067872	Cohort 1
18	F	52	Non-Diabetic	No	373.4086342	8.117579005	Cohort 1
39	F	52	Non-Diabetic	No	51.38008919	1.116958461	Cohort 1
47	M	52	Type 2 Diabetic	Yes	768.3027229	16.70223311	Cohort 2
72	M	52	Non-Diabetic	No	0.864973028	0.018803761	Cohort 1
43	F	53	Non-Diabetic	No	183.9980517	3.999957646	Cohort 1
94	F	53	Non-Diabetic	No	202.6719279	4.405911476	Cohort 1
154	F	53	non-Diabetic	No	17.93962722	0.389991896	Cohort 1
158	M	53	non-Diabetic	No	196.9434107	4.281378494	Cohort 1
73	M	54	Non-Diabetic	No	142.5270775	3.098414728	Cohort 1
168	M	54	Type 2 Diabetic	Yes	92.0612333	2.001331159	Cohort 2
37	M	55	Type 2 Diabetic	Yes	86.11113817	1.871981265	Cohort 2
111	F	55	Type 2 Diabetic	Yes	133.0713687	2.892855841	Cohort 2
21	F	56	Non-Diabetic	No	55.86321062	1.214417622	Cohort 1
122	M	57	Type 2 Diabetic	Yes	138.2169058	3.004715344	Cohort 2
31	M	58	Pre-Diabetic	Yes	448.0842999	9.740963041	Cohort 4
104	M	58	Type 2 Diabetic	Yes	4.436496225	0.09644557	Cohort 2
164	F	58	Type 2 Diabetic	Yes	35.04300608	0.76180448	Cohort 2
5	F	59	Non-Diabetic	No	31.11776644	0.676473183	Cohort 1
34	M	59	Type 1 Diabetic	No	50.06741188	1.088421997	Cohort 1
61	F	61	Non-Diabetic	No	868.1334798	18.87246695	Cohort 1
121	F	61	Type 2 Diabetic	Yes	74.97369122	1.629862853	Cohort 2
173	F	61	non-Diabetic	No	72.93751661	1.585598187	Cohort 1
66	F	62	Non-Diabetic	No	83.74502165	1.820543949	Cohort 1
67	F	63	Non-Diabetic	No	468.9488756	10.19454077	Cohort 1
79	F	63	Non-Diabetic	No	21.03565628	0.457296876	Cohort 1
52	M	64	Type 2 Diabetic	No	82.44886038	1.79236653	Cohort 3
55	F	64	Pre-Diabetic	No	251.7377374	5.472559508	Cohort 1
65	M	64	Type 2 Diabetic	Yes	256.449296	5.574984696	Cohort 2
95	F	64	Non-Diabetic	No	57.26476292	1.244886151	Cohort 1
152	F	64	Type 2 Diabetic	Yes	74.84560351	1.627078337	Cohort 2
51	F	65	Non-Diabetic	No	108.7300275	2.363696249	Cohort 1
117	M	65	Type 2 Diabetic	Yes	293.6872739	6.384505954	Cohort 2
44	F	66	Type 2 Diabetic	Yes	38.72528021	0.841853918	Cohort 2
78	F	66	Type 2 Diabetic	Yes	140.423793	3.052691152	Cohort 2
86	F	66	Non-Diabetic	No	161.2458322	3.505344178	Cohort 1
101	M	66	Type 2 Diabetic	No	9.543999645	0.207478253	Cohort 3

106	F	66	Type 2 Diabetic	Yes	99.52963571	2.163687733	Cohort 2
50	F	67	Type 2 Diabetic	Yes	517.951234	11.25980944	Cohort 2
53	M	67	Non-Diabetic	No	103.8222068	2.257004496	Cohort 1
109	M	67	Type 2 Diabetic	Yes	201.7766782	4.386449527	Cohort 2
110	M	67	Non-Diabetic	No	46.36347555	1.007901642	Cohort 1
48	F	68	Non-Diabetic	No	1077.345597	23.42055646	Cohort 1
99	M	68	Type 2 Diabetic	No	14.80875453	0.321929446	Cohort 3
153	M	68	Type 2 Diabetic	Yes	75.31167564	1.63721034	Cohort 2
171	M	68	Type 2 Diabetic	Yes	82.37271764	1.790711253	Cohort 2
29	F	69	Type 1 Diabetic	No	185.001943	4.02178137	Cohort 1
35	F	69	Type 2 Diabetic	Yes	58.99903793	1.282587781	Cohort 2
38	M	69	Type 2 Diabetic	Yes	104.7606194	2.277404769	Cohort 2
54	M	69	Non-Diabetic	No	150.4813062	3.271332744	Cohort 1
25	F	70	Non-Diabetic	No	294.6918761	6.406345132	Cohort 1
33	F	70	Type 2 Diabetic	Yes	382.8984708	8.3238798	Cohort 2
85	F	70	Non-Diabetic	No	74.30824255	1.615396577	Cohort 1
113	F	70	Type 2 Diabetic	No	67.98111663	1.477850362	Cohort 3
6	F	71	Non-Diabetic	No	3.30541E-09	7.18568E-11	Cohort 1
36	M	71	Type 2 Diabetic	Yes	433.0382444	9.413874879	Cohort 2
45	F	71	Type 2 Diabetic	Yes	818.0051539	17.78272074	Cohort 2
71	M	71	Type 2 Diabetic	Yes	114.5484176	2.490182991	Cohort 2
81	F	71	Non-Diabetic	No	47.08717353	1.023634207	Cohort 1
102	M	71	Type 2 Diabetic	Yes	10.29310794	0.223763216	Cohort 2
112	F	71	Type 2 Diabetic	No	37.79951042	0.821728487	Cohort 3
16	F	72	Type 2 Diabetic	Yes	89.76080684	1.951321888	Cohort 2
26	F	72	Type 2 Diabetic	Yes	50.07815337	1.088655508	Cohort 2
49	M	72	Type 2 Diabetic	No	2987.608101	64.9480022	Cohort 3
62	F	72	Non-Diabetic	No	203.4573999	4.422986953	Cohort 1
64	M	73	Non-Diabetic	No	52.98366356	1.151818773	Cohort 1
69	M	73	Type 2 Diabetic	Yes	12.54978856	0.27282149	Cohort 3
75	M	73	Type 1 Diabetic	No	224.6667548	4.884059887	Cohort 1
80	M	73	Type 2 Diabetic	Yes	69.47639843	1.510356488	Cohort 2
163	F	73	Type 2 Diabetes	Yes	375.9627401	8.173103045	Cohort 2
24	M	74	Type 2 Diabetic	Yes	161.120055	3.502609891	Cohort 2
57	F	74	Type 2 Diabetic	Yes	482.1800237	10.48217443	Cohort 2
107	F	74	Type 2 Diabetic	No	118.1317075	2.568080598	Cohort 3
116	M	74	Type 2 Diabetic	Yes	85.0948733	1.84988855	Cohort 2
41	F	75	Non-Diabetic	No	157.7306675	3.428927555	Cohort 1
46	M	75	Non-Diabetic	No	579.3427487	12.59440758	Cohort 1
60	M	75	Non-Diabetic	No	72.66859806	1.579752132	Cohort 1
90	M	75	Non-Diabetic	No	294.1991839	6.395634433	Cohort 1
119	M	75	Type 2 Diabetes	Yes	649.2852523	14.11489679	Cohort 2
165	F	75	Type 2 Diabetic	Yes	154.0802046	3.349569665	Cohort 2
32	M	76	Type 2 Diabetic	No	370.4981972	8.054308634	Cohort 3

59	F	77	Non-Diabetic	No	475.7960225	10.34339179	Cohort 1
70	M	77	Non-Diabetic	No	144.178518	3.134315609	Cohort 1
63	M	78	Non-Diabetic	No	24.35716339	0.529503552	Cohort 1
96	F	78	Type 2 Diabetic	Yes	2.371553332	0.051555507	Cohort 2
105	M	78	Type 2 Diabetic	Yes	211.2817328	4.593081149	Cohort 2
114	M	79	Type 2 Diabetes	No	56.49806174	1.228218733	Cohort 3
118	M	79	Type 2 Diabetes	Yes	74.36530997	1.616637173	Cohort 2
97	M	80	Type 2 Diabetic	No	25.12856177	0.546273082	Cohort 3
98	M	80	Type 2 Diabetic	Yes	137.2505418	2.98370743	Cohort 2
30	F	81	Type 2 Diabetic	Yes	1121.045761	24.37056001	Cohort 2
56	M	81	Non-Diabetic	No	72.63126282	1.578940496	Cohort 1
19	F	82	Non-Diabetic	No	127.3287525	2.768016359	Cohort 1
174	m	83	Type 2 Diabetic	Yes	266.584888	5.795323652	Cohort 2
58	M	87	Type 2 Diabetic	Yes	177.4161674	3.856873204	Cohort 2
108	M	88	Type 2 Diabetic	Yes	13.35216114	0.290264373	Cohort 2
20	M	96	Non-Diabetic	No	55.66117932	1.210025637	Cohort 1
17	F	100	Type 2 Diabetic	Yes	209.9047454	4.563146639	Cohort 2

3.2 Comparison of age cohorts

Comparison of the mean standard deviation, n-value, and coefficient of variation for the average absolute telomere length in each cohort over the various age ranges for participants over the age of 41 is presented to test our hypothesis. The distribution data necessary for statistical analysis (see Appendix 4) is included in the following three tables (Table 2, 3, and 4). These tables provide the mean standard deviation, n-value, and coefficient of variation for the average absolute telomere length values of Cohort 1 (Table 2), Cohort 2 (Table 3) and Cohort 3 (Table 4) across the ages of 41 to 100. Cohort 4 is not included as there were only two values, both falling within differing age ranges.

The data pertaining to Cohort 1 across defined age ranges shows fluctuating values of mean average absolute telomere length per chromosome, starting with a relatively high value in

the age range of 41-50, decreasing across the 51-60 and 61-70 age range, increasing to its highest mean at the age range of 71-80, and then, finally decreasing in the final two age ranges (Table 2). The standard deviation is quite high for all age ranges, decreasing slightly during the 81-90 age range (Table 2). The coefficient of variation, which compares the standard deviation to the mean stays constant throughout the majority of the age ranges, only decreasing a great deal between the age range of 81-90 (Table 2). The number of individuals between 41 and 80 years of age are all high, ranging from 8 to 14 samples (Table 2). The number of individuals drop considerably after this, with only two data points between the 81-90 age range and a single data point between the 91-100 age range (Table 2).

Table 2:

Table 2: The sample distribution details for the average absolute telomere length per chromosome of the Cohort 1 samples over various age ranges.

Age Range (Years)	**41-50**	**51-60**	**61-70**	**71-80**	**81-90**	**91-100**
Mean	4.08120	2.8389505	3.2303020	4.4989484	2.1734784	1.2100256
Standard Deviation	3.87520	2.4303078	2.6295446	3.9244354	0.8408036	N/A
number	8	10	14	11	2	1
Coefficient of Variation	0.949524	0.8560585	0.8140244	0.8723006	0.3868470	N/A

The data pertaining to Cohort 2 across defined age ranges also shows to have fluctuating values of mean average absolute telomere length per chromosome, with the values beginning moderately, followed by them reaching their peak between the 71-80 age range and then decreasing down to moderate levels between the ages of 81 and 90 (Table 3). The mean value for the age range of 91-100 appears to be the highest, however, it is not a true mean value as it represents only one data point (Table 3). The standard deviation is high for most age ranges, with the first two age ranges having the lowest values (Table 3). The coefficient of variation displayed

a similar trend, with the first two age ranges having the lowest values. n values were low in the 41-50, 81-90, and 91-100 age ranges, moderate in the 51-60 age range, and high in the 61-70 and 71-80 age ranges (Table 3).

Table 3: The sample distribution details for the average absolute telomere length per chromosome of the Cohort 2 samples over various age ranges.

Age Range (Years)	**41-50**	**51-60**	**61-70**	**71-80**	**81-90**	**91-100**
Mean	3.02956	2.1065376	3.3698779	4.2260403	3.3141537	4.5631466
Standard Deviation	1.36002	0.9082142	3.0595772	4.0979523	2.7923696	N/A
number	2	5	16	16	3	1
Coefficient of Variation	0.44892	0.4311407	0.9079193	0.9696908	0.8425588	N/A

The statistical data for Cohort 3 represents the data of two age ranges: 61-70 and 71-80 (Table 4). The mean, standard deviation and number of individuals are both higher in the 71-80 age range than the 61-70 age range (Table 4). However the Coefficient of Variation for both age groups is fairly similar (Table 4).

Table 4: The sample distribution details for the average absolute telomere length per chromosome of the Cohort 3 samples over various age ranges.

Age Range (Years)	**61-70**	**71-80**
Mean	0.7739247	2.643721907
Standard Deviation	0.883851	3.122609933
number	3	5
Coefficient of Variation	1.1420373	1.181141604

3.3 Comparison of telomere lengths between cohorts

The difference in mean average absolute telomere length for each of the four cohorts between the ages of 41 and 100 were compared (Figure 6). The error bars visually display the standard deviation of each sample set (Figure 6). The ‘A’ and ‘B’ values denote p-values

obtained from a t-test (Appendix D). Cohort 4, and anything belonging to the age range of 91-100 do not have error bars because they are single data points (Figure 6). They were included for the sake of completeness, but do not indicate any trends due to the number of individuals. The Cohort 1 mean is noticeably higher than that of Cohort 2 for the first two age ranges (both have B p-values). In the age ranges of 61-70 and 71-80, the means are nearly identical, and both have p-values classified as 'A'. In the age range of 81-90, the mean value of Cohort 2 is noticeably greater than that of Cohort 1. Through the age ranges of 61-70 and 71-80, Cohort 3 has a much smaller mean value than both Cohorts 1 and 2.

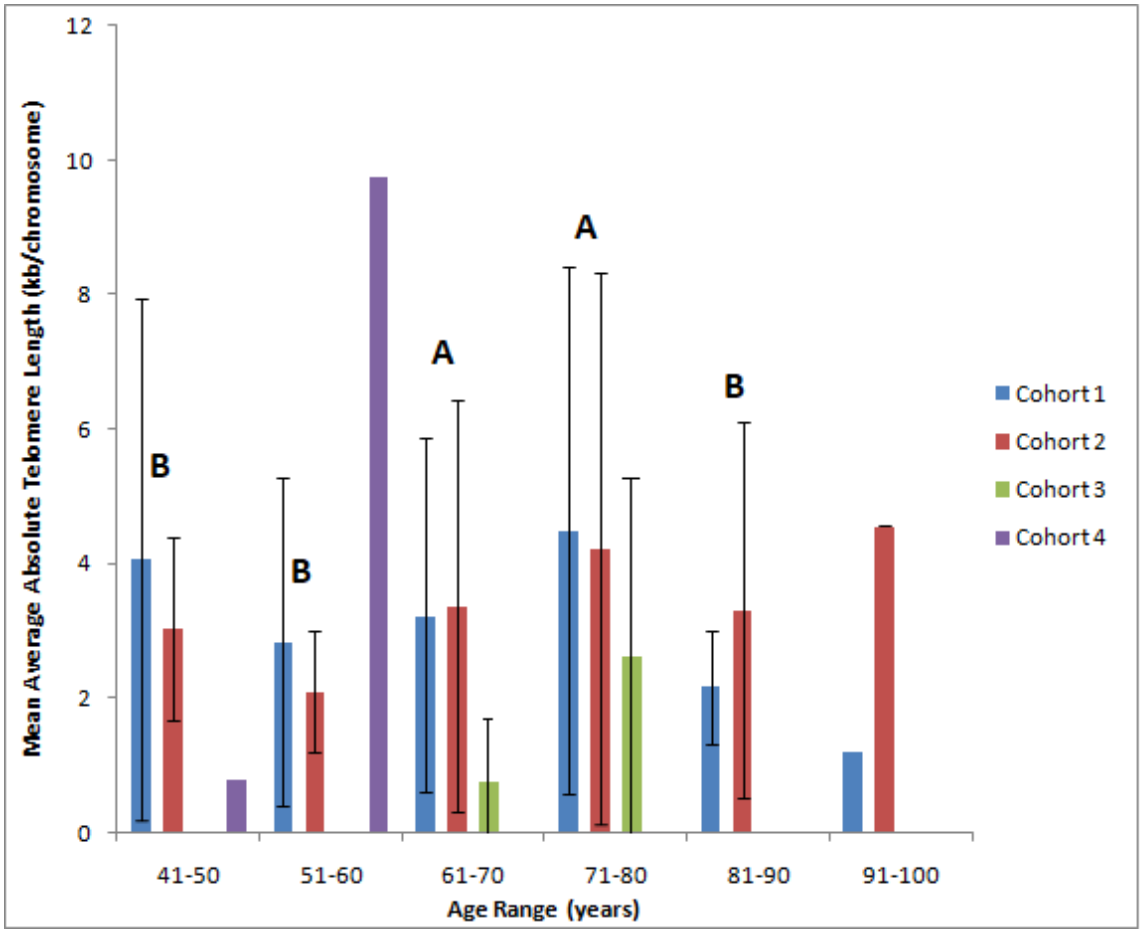

Figure 6: The mean average absolute telomere length per chromosome of Cohort 1, Cohort 2, Cohort 3 and Cohort 4 over time (as shown by age ranges of 10 years).

The legend at the right describes which cohort group corresponds to which bar (Figure 6). T-tests were completed to determine the differences between the mean average absolute telomere length of the Cohort 1and Cohort 2 samples. The 'A' indicates a p-value between 0.4 and 0.5 and a 'B' indicates a p-value between 0.2 and 0.3 (Figure 6). Error bars indicating standard deviation were included for the Cohort 1 and Cohort 2 samples (Figure 6). Error bars were not generated for Cohort 1 and Cohort 2 samples which fell into the age range of 91-100, as there was only one data point for each (Figure 6). Similarly, error bars were not included for the Cohort 4 samples as there was only a single data point in two separate age ranges (Figure 6).

3.4 Statistical Analysis

Statistical analyses were completed to test for statistically significant differences in the sets of average absolute telomere length data between cohort groups.

Linear regression analysis was completed using IBM SPSS Statistics Data Editor for Cohort 1 (Table 5), Cohort 2 (Table 6), and Cohort 3 (Table 7) to determine if age impacted the average absolute telomere length for these cohort groups. It was found that, through the analysis of all three linear regression models, age does not have a statistically significant impact (a p-value greater than 0.05) on the average absolute telomere length. Because of this, age was not determined to be a covariant factor, and an ANCOVA test was not completed for the data.

Table 5: The model summary for the regression model analysis showing the impact age has on average absolute telomere length in the Cohort 1 data set.

Model Summary[b]

Model	R	R Square	Adjusted R Square	Std. Error of the Estimate	Change Statistics				
					R Square Change	F Change	df1	df2	Sig. F Change
1	.006[a]	.000	-.023	3.128669	.000	.002	1	44	.967

a. Predictors: (Constant), Age

b. Dependent Variable: Average Absolute Telomere Length per Chromosome

The regression analysis between age and average absolute telomere length for Cohort 1 (Table 5) shows that age does not have a significant impact on that average absolute telomere length, giving a p-value of 0.967 (a value higher than 0.05). Both the R Square value and the adjusted R Square value show that 0% of the variance in the average absolute telomere length is determined by the age.

Table 6: The model summary for the regression model analysis showing the impact age has on average absolute telomere length in the Cohort 2 data set.

Model Summary[b]

Model	R	R Square	Adjusted R Square	Std. Error of the Estimate	Change Statistics				
					R Square Change	F Change	df1	df2	Sig. F Change
1	.139[a]	.019	-.005	3.2184465	.019	.806	1	41	.375

a. Predictors: (Constant), Age (years)

b. Dependent Variable: Average Absolute Telomere Length per Chromosome

The regression analysis between age and average absolute telomere length for Cohort 2 (Table 6) shows that age does not have a significant impact on that average absolute telomere length,

giving a p-value of 0.375 (a value higher than 0.05). The R Square value indicates that 1.9% of the variance in the average absolute telomere length is determined by the age. The adjusted R Square value indicates that 0% of the variance in the average absolute telomere length is determined by the age.

Table 7: The model summary for the regression model analysis showing the impact age has on average absolute telomere length in the Cohort 3 data set.

Model Summary[b]

					Change Statistics				
Model	R	R Square	Adjusted R Square	Std. Error of the Estimate	R Square Change	F Change	df1	df2	Sig. F Change
1	.265[a]	.070	-.085	2.702135336001004	.070	.453	1	6	.526

a. Predictors: (Constant), Age (Years)

b. Dependent Variable: Average Absolute Telomere Length per Chromosome

The regression analysis between age and average absolute telomere length for Cohort 3 (Table 7) shows that age does not have a significant impact on that average absolute telomere length, giving a p-value of 0.526 (a value higher than 0.05). The R Square value indicates that 7% of the variance in the average absolute telomere length is determined by the age. The adjusted R Square value indicates that 0% of the variance in the average absolute telomere length is determined by the age

Two-tailed t-tests were completed using Microsoft Excel 2016 to test for a statistically significant difference between the average absolute telomere length data in each cohort group.

Table 8: T-Test analysis comparing the statistical difference of the average absolute telomere length between Cohort 1 and Cohort 2.

Age range	p-values
41-50	0.276919834
51-60	0.207630726
61-70	0.447034948
71-80	0.431576712
81-90	0.281522037
91-100	N/A

The t-test analysis comparing Cohort 1 and Cohort 2 values (Table 8) did not generate any p-values below 0.05, indicating no statistically significant difference between these sets of data.

Table 9: T-Test analysis comparing the statistical difference of the average absolute telomere length between Cohort 1 and Cohort 3.

Age Range	p-values
61-70	0.008344497
71-80	0.167591622

The t-test analysis comparing Cohort 1 and Cohort 3 values between the age ranges of 61-70 and 71-80 (Table 9) showed a p-value less than 0.05 for the age range of 61-70. This potentially indicates a statistically significant difference between these two cohorts for that age range. The p-value for these two cohorts between the age range of 71-80 was greater than 0.05, indicating no statistically significant difference between the data sets for this age range.

Table 10: T-Test analysis comparing the statistical difference of the average absolute telomere length between Cohort 2 and Cohort 3.

Age Range	p-values
61-70	0.007374206
71-80	0.192657552

The t-test analysis comparing Cohort 2 and Cohort 3 between the ages of 61-70 and 71-80 (Table 9) displays a p-value less than 0.05 for the age range of 61-70. This could indicate a statistically significant difference between these two cohorts for that age range. Conversely, the p-value for these two cohorts between the ages of 71-80 was greater than 0.05, indicating no statistically significant difference between the cohort groups for this age range.

Table 11: A one-way ANOVA test comparing the statistical difference of the average absolute telomere length between Cohort 1, Cohort 2 and Cohort 3.

ANOVA summary	
F	0.008366
P value	0.9917
P value summary	ns
Significant diff. among means (P < 0.05)?	No
R square	0.0005574

The ANOVA test summarized in Table 11 was created using GraphPad Prism 7.05. The p-value obtained was 0.9917 (larger than 0.05), indicating the absence of a statistical difference for the average absolute telomere lengths between Cohort 1, Cohort 2 and Cohort 3.

3.5 Method Verification

The methods were evaluated using controls, standards and quantification. All controls and standards were run with every qPCR. If any of the extraction negative and qPCR negative controls were deemed compromised the analysis was repeated. The standards used for calculation purposes were amplified on the same plate at the test samples so that a standard curve could be determined for every run since there is the possibility for inter-run variability. All extractions were quantified to ensure the appropriate amount of DNA was added to each reaction

as optimized. Some of the samples were randomly checked for inter-run variability by replication (Table 5). For example the average absolute telomere length for the same sample across two separate qPCR amplifications (Table 5). The values run on both dates are both very similar.

Table 12: A comparison of qPCR results for the same unknown sample extracted and purified separately and analyzed through separate qPCR amplifications.

Sample	Absolute telomere length per genome (kb/genome)	Average absolute telomere length per chromosome (kb/chromosome)	Date Run
58	177.4161674	3.856873204	August 5, 2018
58	172.7206381	3.75479648	August 24, 2018

The average absolute telomere lengths for both analyses of sample 58 (on August 5th, 2018 and August 24, 2018) were quite similar to one another, having a percent difference of only 2.89% (Table 12).

4 Discussion

4.1 Precision and accuracy of results

There were relatively high standard deviations in this data when comparing the coefficient of variation to their means (Table 2-4 and Figure 6). This indicates a large spread of data points and low precision for most of the age ranges of the data. This result is likely due to the complexity and number of factors that affect the rate of telomere shortening. Due to the limited sample size, the results were organized by age ranges of ten years and were not further subdivided by sex, ethnic origin, health, caloric intake, lifestyle, duration of treatment, or treatment dose even though there is evidence that all these factors affect telomere shortening (77, 85, 84, 11, 9). The varying combinations of these factors in the tested individuals is what could have led to this large standard deviation. This, along with some slight variability of the qPCR method could have been the reason for the diverse range in data.

Although the methodology is consistent with other studies, it would have contributed to some degree of imprecision, as telomere analysis via qPCR has a variability between 5-10% (50). This effect, however, seems to be minimal as repeated analysis of the same unknown sample led to very highly similar results (Table 5).

Comparing the data generated in this study to literature values can assist in determining accuracy of the data itself. The mean average absolute telomere length for Cohort 1 and 2 range from below 5 kb/chromosome to above 2 kb/chromosome (Figure 6). This is similar, albeit slightly lower, than the values obtained from other studies (77, 78). Frenck *et al*. (78) found that, between an individual's early 40s and late 70s, telomere length decreased from around 10.5 to 8 kb/chromosome. Findings from Bischoff *et al*. (77), combined with data from Benetos *et al*. (41) indicate telomere length from whole blood decreases from 8.5 to 7.5 kb/chromosome between an

individual's early 40s and late 70s. Although some samples were obtained from healthy individuals who were simply interested in participating in the study, many of the participants were recruited from Curans Heart Centre, a clinic for individuals with cardiac health concerns. Research has shown that cardiovascular diseases can result in increased telomere attrition (79). Particularly, heart conditions such as artery stiffness, the advanced stages of atherosclerosis, and coronary heart disease have all been found to cause an increased rate of telomere shortening (80, 81, 82). Perhaps this could explain why the average absolute telomere length was slightly lower than expected. This could also be a possible explanation for the high variation of data. The results of this study show a slight decrease in Cohort 1's average absolute telomere length over time from the age of 41 to 100 (Table 2 and Figure 6). This does follow the expected trend of a gradual decrease in telomere length from young adulthood to old age (78). The control group displaying the expected gradual attrition in telomere length does lend further support to the accuracy of the results.

4.2 The effects of metformin use on average absolute telomere length

In the earlier age ranges (41-50, and 51-60), the mean average absolute telomere length for Cohort 2 begins by being noticeably lower than the mean average absolute telomere length of Cohort 1 (Table 2, 3 and Figure 6). However, in the age ranges of 61-70 and 71-80, the mean average absolute telomere length for both Cohort 1 and 2 are nearly the same, indicating a relatively slower decrease in telomere length for Cohort 2 with advanced age when compared to the negative control (Table 2, 3 and Figure 6). This can be seen further in the 81-90 and 91-100 age ranges in which the mean average absolute telomere length of Cohort 2 is noticeably higher than that of Cohort 1 (Table 2, 3 and Figure 6). It should be noted that these last two age ranges

have few data points (2 for Cohort 1 and 3 for Cohort 3 in the 81-90 age range, and 1 each for the 91-100 age range), so any conclusions relating to individuals over the age of 80 is more suspect than that of the younger age ranges.

This relative slowing of telomere attrition in Cohort 2 could be due, in part, to the duration of metformin treatment. It has been shown in previous research that metformin is most effective at improving longevity with extended treatments (11). This could explain why telomere attrition in Cohort 2 slowed with age relative to the negative control. After the age of 45-50, the risk for developing type 2 diabetes increases (45). It could be inferred that most patients were likely diagnosed with type 2 diabetes during middle age and would have started the first-line metformin treatment around this age, resulting in Cohort 2 having relatively longer mean average absolute telomere lengths as time progressed and more years were spent taking the drug. Although these trends appear to be present through visual interpretation of Figure 6, the statistical t-tests did not show any statistical difference between the data from Cohort 1 and 2 (Table 8). This was likely due to the relatively large spread in data points and subsequent large standard deviations (Table 2, Table 3). However, Cohort 3 has a considerably lower mean average absolute telomere length than both Cohort 1 and 2 (Table 2-4). For the age range of 61-70, the t-test values seem to indicate that there is a significant difference between both Cohorts 1 and 3, and Cohorts 2 and 3, with p-values of 0.0083 and 0.0074 respectively (Table 9, Table 10). The differences in mean average absolute telomere length for the age range of 71-80 did not show statistically significant values, giving p-values of 0.167591633 and 0.192657552 for Cohort 1 and Cohort 3 respectively (Table 9, Table 10).

The one-way ANOVA test (Table 11), which compared all three cohort groups along the age range of 61-70, provided results which conflicted with the t-tests in Table 9 and Table 10.

This ANOVA test did not find a statistically significant difference between the three cohorts for the age range of 61-70 (Table 11). This discrepancy could be present because the one-way ANOVA test compares all three means against each other simultaneously, whereas both t-tests specifically compared Cohort 3 with Cohorts 1 and 2 separately. Perhaps the one-way ANOVA test was not able to register a statistically significant difference due to the variance of all three datasets, yet differences between the two cohorts exist. It is also possible the statistically significant p-values obtained from the t-tests were false positives (type I error).

Overall, it appears that there might be some evidence to support the notion that the mean average absolute telomere length for diabetics not taking metformin is lower than the mean average absolute telomere length for type 2 diabetics taking metformin as well as healthy control samples. However, due to conflicting statistical analyses and the fact that this trend is only observed within a ten year age range, no definitive conclusions can be made at this time.

4.3 Study limitations and future directions

A limitation with this study is the relatively low sample size, specifically for Cohorts 3 and 4. With greater numbers of samples from these two cohort groups, a more balanced study could be undertaken, proving more definitive conclusions about metformin's effect on telomere length. It is likely that our relatively small numbers of individuals in each age group were not large enough to resolve the differences in telomere length seen in the previous studies with their hundreds of subjects. In future studies it might be pertinent to selectively recruit participants of similar sex, ethnic origin, health status, length of treatment, and dosage. Improved control of these external variables could result in more precise findings.

It may also prove useful, in future studies, to explore alternative analytical techniques for analyzing telomeres. The qPCR method is known to have a high degree of variability within its final results, lending to a higher variance of the data. Perhaps a method such as the Southern Blot technique, which is highly reproducible and considered to be quite precise, would be a more suitable option (93, 94).

5 Conclusion

Although this preliminary study was able to identify several trends in how metformin and type 2 diabetes can affect telomere length, a conclusive link between metformin use and telomere length is still yet to be firmly established. All calculated telomere lengths were reasonable when compared to other published works, however, due to high standard deviations, statistical significance was not established between type 2 diabetics taking metformin (Cohort 2) and negative control samples (Cohort 1). Despite this, the mean average absolute telomere length did appear to have a decrease in its attrition rate when compared to the negative control values. This led to the mean average absolute telomere length of Cohort 2 matching and later surpassing the Cohort 1 levels with age.

There did, however, appear to be a difference in average absolute telomere length between type 2 diabetics not taking metformin (Cohort 3) and Cohorts 1 and 2. Cohort 3 appeared to have a reduced mean average absolute telomere length when compared to both Cohort 1 and Cohort 2. This lower telomere length in Cohort 3 when compared to Cohort 2 indicates that metformin use may slow the process of telomere shortening in older adults. However, although t-testing indicates that this was statistically significant between the age of 71-

80, one-way ANOVA testing showed no statistical difference between all three cohorts. Because of this, no definitive links between metformin and telomere length can be stated.

To determine more definitive results, a greater amount of data would likely need to be collected and balanced more evenly across the four cohort groups. To improve specificity, it may be prudent for future studies in this area to factor in variables such as sex, ethnic origin, exercise, caloric intake, lifestyle, health, metformin treatment length, and metformin dosage. It may also be useful to measure telomere length through alternative analytical techniques such as the Southern blot technique to compare and validate the measurement methods employed. Overall, this evidence from this study does hint at possible geroprotective effects for metformin, and would warrant further in-depth studies in the future.

6 References

1) Viollet, B., Guigas, B., Garcia, N.S., Leclerc, J., Foretz, M. and Andreelli, F. Cellular and molecular mechanisms of metformin: an overview. *Clinical science*, 122(6), 253-270, 2012.
2) Zhou, G., Myers, R., Li, Y., Chen, Y., Shen, X., Fenyk-Melody, J., Wu, M., Ventre, J., Doebber, T., Fujii, N., Musi, N., Hirshman, M., Goodyear, L. and Moller, D. Role of AMP-activated protein kinase in mechanism of metformin action. *The Journal of Clinical Investigation*, 108: 1167-1174, 2001.
3) Bailey, C.J., Mynett, K.J. and Page, T. Importance of the intestine as a site of metformin-stimulated glucose utilization. *Brazilian Journal of Pharmacology*, 112: 671-675, 1994.

4) Bailey, C.J., Wilcock, C. and Scarpello, J.H. Metformin and the intestine. *Diabetologia*, 51: 1552–1553, 2008.

5) Masoro, E. Overview of caloric restriction and ageing. *Mechanisms of Ageing and Development*, 126: 913-922, 2005.

6) Spindler, S. Caloric Restriction: From soup to nuts. *Ageing Research Reviews*, 9: 324-353, 2010.

7) Johnson, S.C., Rabinovitch, P.S. and Kaeberlein, M. mTOR is a key modulator of ageing and age-related disease. *Nature*, 493: 338-345, 2013.

8) Anisimov, V.N. and Bartke, A. The key role of growth hormone-insulin-IGF-1 signaling in aging and cancer. *Critical Review of Oncology and Hematology*, 87(3): 201-223, 2013.

9) Martin-Montalvo, A., Mercken, E., et al. Metformin improves healthspan and lifespan in mice. *Nature Communications*, 4(1): 2192, 2013.

10) DeFronzo, R., Fleming, A., Chen, K. and Bicsak, T. Metformin-associated lactic acidosis: Current perspectives on causes and risk. *Metabolism*, 65(2): 20-29, 2016.

11) Anisimov, V.N., Berstein, L.M., Popovich, I.G., Zabezhinski, M.A., Egormin, P.A., Piskunova, T.S., Semenchenko, A.V., Tyndyk, M.L., Yurova, M.N., Kovalenko, I.G. and Poroshina, T.E. If started early in life, metformin treatment increases life span and postpones tumors in female SHR mice. *Aging*, 3: 148-157, 2011.

12) Anisimov, V.N., Berstein, L.M., Egormin, P.A., Piskunova, T.S., Popovich, I.G., Zabezhinski, M.A., Tyndyk, M.L., Yurova, M.V., Kovalenko, I.G., Poroshina, T.E., et al. Metformin slows down aging and extends lifespan of female SHR mice. *Cell Cycle*, 7: 2769-2773, 2008.

13) Anisimov, V.N., Berstein, L.M,, Egormin, P.A., Piskunova, T.S., Popovich, I.G., Zabezhinski, M.A., Kovalenko, I.G., Poroshina, T.E., Semenchenko, A.V., Provinciali, M., et al. Effect of metformin on lifespan and on the development of spontaneous mammary tumors in HER-2/ neu transgenic mice. *Experimental Gerontology*, 40: 685-693, 2005.

14) Anisimov, V.N., Egormin, P.A., Piskunova, T.S., Popovich, I.G., Tyndyk, M.L., Yurova, M.N., Zabezhinski, M.A., Anikin, I.V., Karkach, A.S. and Romanyukha, A.A. Metformin extends lifespan of HER-2/neu transgenic mice and in combination with melatonin inhibits growth of transplantable tumors in vivo. *Cell Cycle*, 9: 188-197, 2010.

15) Anisimov, V.N., Piskunova, T.S., Popovich, I.G., Zabezhinski, M.A., Tyndyk, M.L., Egormin, P.A., Yurova, M.V., Rosenfeld, S.V., Semenchenko, A.V., Kovalenko, I.G., et al. Gender differences in metformin effect on aging, lifespan and spontaneous tumorigenesis in 129/Sv mice. *Aging*, 2: 945-958, 2010.

16) Onken, B. and Driscoll, M. Metformin induces a dietary restriction-like state and the oxidative stress response to extend *C. elegans* healthspan via AMPK, LKB1, and SKN-1. *PLoS ONE5*, e8758, 2010.

17) Cabreiro, F., Au, C., Leung, K., Vergara-Irigaray, N., Cocheme, H., Noori, T., Weinkove, D., Schuster, E., Greene, D. and Gems, D. Metformin Retards Aging in *C. elegans* by Altering Microbial Folate and Methionine Metabolism. *Cell*, 153: 228-239, 2013.

18) Nakayama, J. I., Tahara, H., Tahara, E., Saito, M., Ito, K., Nakamura, H., ... & Ishikawa, F. Telomerase activation by hTRT in human normal fibroblasts and hepatocellular carcinomas. Nature genetics: 18(1), 65. 1998

19) Vaziri, H., & Benchimol, S. Reconstitution of telomerase activity in normal human cells leads to elongation of telomeres and extended replicative life span. Current Biology, 8(5): 279-282. 1998

20) Linden, M.A., Lopez, K.T., Fletcher, J.A., Morris, E.M., Meers, G.M., Siddique, S., ... and Rector, R.S. Combining metformin therapy with caloric restriction for the management of type 2 diabetes and nonalcoholic fatty liver disease in obese rats. *Applied Physiology, Nutrition, and Metabolism*, 40(10): 1038-1047, 2015.

21) Mazza, A., Fruci, B., Garinis, G.A., Giuliano, S., Malaguarnera, R., and Belfiore, A. The role of metformin in the management of NAFLD. *Experimental diabetes research*, 2012, 2011

22) Zhang, S., Liu, X., Brickman, W.J., Christoffel, K.K., Zimmerman, D., Tsai, H.J., ... and Liu, X. Association of plasma leptin concentrations with adiposity measurements in rural Chinese adolescents. *The Journal of Clinical Endocrinology and Metabolism*, 94(9): 3497-3504, 2009.

23) Blagosklonny, M.V. Validation of anti-aging drugs by treating age-related diseases. *Aging*, 1(3): 281, 2009.

24) Sohal, R.S., and Weindruch, R. Oxidative stress, caloric restriction, and aging. *Science*, 273(5271): 59-63, 1996.

25) Gonzales-Pacheco, D.M., Buss, W.C., Koehler, K.M., Woodside, W.F., and Alpert, S.S. . Energy restriction reduces metabolic rate in adult male Fisher-344 rats. *The Journal of nutrition*, 123(1): 90-97, 1993.

26) Duffy, P.H., Feuers, R., Nakamura, K.D., Leakey, J., and Hart, R.W. Effect of chronic caloric restriction on the synchronization of various physiological measures in old female Fischer 344 rats. *Chronobiology international*, 7(2): 113-124, 1990.

27) Weindruch, R. and Walford, R.L. *Retardation of aging and disease by dietary restriction*. CC Thomas, 1988.

28) Rabbani, N., Chittari, M.V., Bodmer, C.W., Zehnder, D., Ceriello, A., and Thornalley, P.J. Increased glycation and oxidative damage to apolipoprotein B100 of LDL in patients with type 2 diabetes and effect of metformin. *Diabetes*, 2010.

29) Algire, C., Moiseeva, O., Deschênes-Simard, X., Amrein, L., Petruccelli, L., Birman, E., ... and Pollak, M.N. Metformin reduces endogenous reactive oxygen species and associated DNA damage. *Cancer Prevention Research*, 2012

30) Zhao, R.R., Xu, X. C., Xu, F., Zhang, W.L., Zhang, W.L., Liu, L.M., and Wang, W.P. Metformin protects against seizures, learning and memory impairments and oxidative damage induced by pentylenetetrazole-induced kindling in mice. *Biochemical and biophysical research communications*, 448(4): 414-417, 2014.

31) El-Mir, M.Y., Detaille, D., Gloria, R., Delgado-Esteban, M., Guigas, B., Attia, S., ... and Leverve, X. Neuroprotective role of antidiabetic drug metformin against apoptotic cell death in primary cortical neurons. *Journal of Molecular Neuroscience*, 34(1): 77-87, 2008.

32) El-Mir, M.Y., Detaille, D., Gloria, R., Delgado-Esteban, M., Guigas, B., Attia, S., ... and Leverve, X. Neuroprotective role of antidiabetic drug metformin against apoptotic cell death in primary cortical neurons. *Journal of Molecular Neuroscience*, 34(1): 77-87, 2008.

33) Mousavi, S.M., Niazmand, S., Hosseini, M., Hassanzadeh, Z., Sadeghnia, H.R., Vafaee, F., and Keshavarzi, Z. Beneficial effects of Teucriumpolium and metformin on diabetes-induced memory impairments and brain tissue oxidative damage in rats. *International Journal of Alzheimer's Disease*, 2015

34) Ashabi, G., Khodagholi, F., Khalaj, L., Goudarzvand, M., and Nasiri, M. Activation of AMP-activated protein kinase by metformin protects against global cerebral ischemia in male rats: Interference of AMPK/PGC-1α pathway. *Metabolic brain disease*, 29(1): 47-58, 2014.

35) O'Callaghan, N.J. and Fenech, M.A. quantitative PCR method for measuring absolute telomere length. *Biological procedures online*, 13(1): 2011.

36) Rudolph, K.L. (Ed.). *Telomeres and Telomerase in Ageing, Disease, and Cancer: Molecular Mechanisms of Adult Stem Cell Ageing*. Berlin, Springer, 2008.

37) Baird, D.M. and Kipling, D. The extent and significance of telomere loss with age. *Annals of the New York Academy of Sciences*, 1019(1): 265-268, 2004.

38) Blackburn, E.H. Structure and function of telomeres. *Nature*, 350(6319): 569-573, 1991.

39) Levy, M.Z., Allsopp, R.C., Futcher, A.B., Greider, C.W. and Harley, C.B. Telomere end-replication problem and cell aging. *Journal of molecular biology*, 225(4): 951-960, 1992.

40) Sanders, J.L. and Newman, A.B. Telomere length in epidemiology: a biomarker of aging, age-related disease, both, or neither? *Epidemiologic reviews*:, 2013.

41) Benetos, A., Okuda, K., Lajemi, M., Kimura, M., Thomas, F., Skurnick, J., ... and Aviv, A. Telomere length as an indicator of biological aging. *Hypertension*, 37(2): 381-385, 2001.

42) deKreutzenberg, S.V., Ceolotto, G., Cattelan, A., Pagnin, E., Mazzucato, M., Garagnani, P., ... and Avogaro, A. Metformin improves putative longevity effectors in peripheral mononuclear cells from subjects with prediabetes. A randomized controlled trial. *Nutrition, Metabolism and Cardiovascular Diseases*, 25(7): 686-693, 2015.

43) Kejariwal, D., Stepien, K.M., Smith, T., Kennedy, H., Hughes, D.A. and Sampson, M.J. Lack of association of colonic epithelium telomere length and oxidative DNA damage in Type 2 diabetes under good metabolic control. *BMC endocrine disorders*, 8(1): 12, 2008.

44) Zhou, X.Z., Xue, Y.M., Zhu, B. and Sha, J.P. Effects of metformin on proliferation of human colon carcinoma cell line SW-480. *Journal of Southern Medical University*, 30(8): 1935-1938, 2010.

45) Bodnar, A.G., Ouellette, M., Frolkis, M., Holt, S.E., Chiu, C.P., Morin, G.B., ... and Wright, W.E. Extension of life-span by introduction of telomerase into normal human cells. *Science*, 279(5349): 349-352, 1998.

46) Cantrell, L.A., Zhou, C., Mendivil, A., Malloy, K.M., Gehrig, P.A. and Bae-Jump, V.L. Metformin is a potent inhibitor of endometrial cancer cell proliferation - implications for a novel treatment strategy. *Gynecologic oncology*,116(1): 92-98, 2010.

47) Hanna, R.K., Zhou, C., Malloy, K.M., Sun, L., Zhong, Y., Gehrig, P.A. and Bae-Jump, V.L. Metformin potentiates the effects of paclitaxel in endometrial cancer cells through inhibition of cell proliferation and modulation of the mTOR pathway. *Gynecologic oncology*, 125(2): 458-469, 2012.

48) American Diabetes Association. Diagnosis and classification of diabetes mellitus. *Diabetes care*, 37(Supplement 1), S81-S90, 2014.

49) Bailey, C J. Metformin: historical overview. *Diabetologia*, 60(9): 1566-1576, 2017.

50) Werner, E.A. and Bell, J. CCXIV - The preparation of methylguanidine, and of ββ-dimethylguanidine by the interaction of dicyanodiamide and methylammonium and dimethylammonium chlorides respectively. *Journal of the Chemical Society, Transactions*, 121: 1790-1794, 1922.

51) Luft, D., Schmülling, R.M. and Eggstein, M. Lactic acidosis in biguanide-treated diabetics. *Diabetologia*, 14(2): 75-87, 1978.

52) Lalau, J.D. Lactic acidosis induced by metformin. *Drug safety*, 33(9): 727-740, 2010.

53) Lucis, O.J. The status of metformin in Canada. *Canadian Medical Association Journal*, 128(1): 24, 1983.

54) UK Prospective Diabetes Study (UKPDS) Group. Effect of intensive blood-glucose control with metformin on complications in overweight patients with type 2 diabetes (UKPDS 34). *The Lancet*, 352(9131): 854-865, 1998.

55) Rena, G., Pearson, E.R. and Sakamoto, K. Molecular mechanism of action of metformin: old or new insights? *Diabetologia*, 56(9): 1898-1906, 2013.

56) Nathan, D.M., Buse, J.B., Davidson, M.B., Heine, R.J., Holman, R.R., Sherwin, R. and Zinman, B. Management of hyperglycaemia in type 2 diabetes: a consensus algorithm for the initiation and adjustment of therapy. *Diabetologia*, 49(8): 1711-1721, 2006.

57) Rodbard, H., Jellinger, P., Davidson, J., Einhorn, D., Garber, A., Grunberger, G., ... and Moghissi, E. Statement by an American Association of Clinical Endocrinologists/American College of Endocrinology consensus panel on type 2 diabetes mellitus: an algorithm for glycemic control. *Endocrine practice*, 15(6): 540-559, 2009.

58) Inzucchi, S.E., Bergenstal, R.M., Buse, J.B., Diamant, M., Ferrannini, E., Nauck, M., ... and Matthews, D.R. Management of hyperglycaemia in type 2 diabetes: a patient-centered approach. Position statement of the American Diabetes Association (ADA) and the European Association for the Study of Diabetes (EASD). *Diabetologia*, 55(6): 1577-1596, 2012.

59) He, L. and Wondisford, F.E. Metformin action: concentrations matter. *Cell metabolism*, 21(2): 159-162, 2015.

60) Hardie, D.G. and Carling, D. The AMP-activated protein kinase: Fuel gauge of the mammalian cell? *European journal of biochemistry*, 246(2): 259-273, 1997.

61) Morales, D.R. and Morris, A.D. Metformin in cancer treatment and prevention. *Annual review of medicine*, 66: 17-29, 2015.

62) Sachdev, D. and Yee, D. Disrupting insulin-like growth factor signaling as a potential cancer therapy. *Molecular cancer therapeutics*, 6(1): 1-12, 2007.

63) Kalaany, N.Y. and Sabatini, D.M. Tumours with PI3K activation are resistant to dietary restriction. *Nature*, 458(7239): 725, 2009.

64) Fendt, S.M., Bell, E.L., Keibler, M.A., Davidson, S.M., Wirth, G.J., Fiske, B., ... and Patnaik, A. Metformin decreases glucose oxidation and increases the dependency of prostate cancer cells on reductive glutamine metabolism. *Cancer research*, 2013

65) Garrett, C.R., Hassabo, H.M., Bhadkamkar, N.A., Wen, S., Baladandayuthapani, V., Kee, B.K., ... and Hassan, M.M. Survival advantage observed with the use of metformin in patients with type II diabetes and colorectal cancer. *British journal of cancer*, 106(8): 1374, 2012.

66) Sadeghi, N., Abbruzzese, J.L., Yeung, S.C.J., Hassan, M. and Li, D. Metformin use is associated with better survival of diabetic patients with pancreatic cancer. *Clinical cancer research*, 2012.

67) Currie, C.J., Poole, C.D., Jenkins-Jones, S., Gale, E.A., Johnson, J.A. and Morgan, C.L. Mortality after incident cancer in people with and without type 2 diabetes: impact of metformin on survival. *Diabetes care*, DC_111313, 2012.

68) Hou, G., Zhang, S., Zhang, X., Wang, P., Hao, X. and Zhang, J. Clinical pathological characteristics and prognostic analysis of 1,013 breast cancer patients with diabetes. *Breast cancer research and treatment*, 137(3): 807-816, 2013.

69) Asensio-López, M.C., Lax, A., Pascual-Figal, D.A., Valdés, M. and Sánchez-Más, J. Metformin protects against doxorubicin-induced cardiotoxicity: involvement of the

adiponectin cardiac system. *Free Radical Biology and Medicine*, 51(10): 1861-1871, 2011.

70) Chang, J., Jung, H.H., Yang, J.Y., Lee, S., Choi, J., Im, G.J. and Chae, S.W. Protective effect of metformin against cisplatin-induced ototoxicity in an auditory cell line. *Journal of the Association for Research in Otolaryngology*, 15(2): 149-158, 2014.

71) Knowler, W.C., Barrett-Connor, E., Fowler, S.E., Hamman, R.F., Lachin, J.M., Walker, E.A. and Nathan, D.M. Reduction in the incidence of type 2 diabetes with lifestyle intervention or metformin. *The New England journal of medicine*, 346(6): 393-403, 2002.

72) McDonagh, M.S., Selph, S., Ozpinar, A. and Foley, C. Systematic review of the benefits and risks of metformin in treating obesity in children aged 18 years and younger. *JAMA pediatrics*, 168(2): 178-184, 2014.

73) Velazquez, E.M., Mendoza, S., Hamer, T., Sosa, F. and Glueck, C.J. Metformin therapy in polycystic ovary syndrome reduces hyperinsulinemia, insulin resistance, hyperandrogenemia, and systolic blood pressure, while facilitating normal menses and pregnancy. *Metabolism-Clinical and Experimental*, 43(5): 647-654, 1994.

74) Lord, J.M., Flight, I.H. and Norman, R.J. Metformin in polycystic ovary syndrome: systematic review and meta-analysis. *British Medical Journal*, 327(7421): 951, 2003.

75) Birben, E., Sahiner, U.M., Sackesen, C., Erzurum, S. and Kalayci, O. Oxidative stress and antioxidant defense. *World Allergy Organization Journal*, 5(1): 9, 2012.

76) Invitrogen LentiArray Human CRISPR ... - assets.fishersci.com. (n.d.). Retrieved from https://assets.fishersci.com/TFS-

Assets/LSG/manuals/MAN0016074_LentiArray_Human_CRISPR_Library_Glycerol_Stocks_UG.pdf

77) Bischoff, C., Graakjaer, J., Petersen, H.C., Jeune, B., Bohr, V.A., Koelvraa, S. and Christensen, K. Telomere length among the elderly and oldest-old. *Twin Research and Human Genetics*, 8(5): 425-432, 2005.

78) Frenck, R.W., Blackburn, E.H. and Shannon, K.M. The rate of telomere sequence loss in human leukocytes varies with age. *Proceedings of the National Academy of Sciences*, 95(10): 5607-5610; 1998.

79) Fitzpatrick, A.L., Kronmal, R.A., Gardner, J.P., Psaty, B.M., Jenny, N.S., Tracy, R.P., ... and Aviv, A. Leukocyte telomere length and cardiovascular disease in the cardiovascular health study. *American journal of epidemiology*, 165(1): 14-21, 2006.

80) Kilian, A., Bowtell, D. D., Abud, H. E., Hime, G. R., Venter, D. J., Keese, P. K., ... & Jefferson, R. A. Isolation of a candidate human telomerase catalytic subunit gene, which reveals complex splicing patterns in different cell types. Human molecular genetics: 6(12), 2011-2019. 1997

81) Willeit, P., Willeit, J., Brandstätter, A., Ehrlenbach, S., Mayr, A., Gasperi, A., ... and Kiechl, S. Cellular aging reflected by leukocyte telomere length predicts advanced atherosclerosis and cardiovascular disease risk. *Arteriosclerosis, thrombosis, and vascular biology*, 30(8): 1649-1656, 2010.

82) Haycock, P.C., Heydon, E.E., Kaptoge, S., Butterworth, A.S., Thompson, A., and Willeit, P. Leucocyte telomere length and risk of cardiovascular disease: systematic review and meta-analysis. *British Medical Journal*, 349, g4227, 2014.

83) Human Cell, Chromosome and Telomere Stock Vector - Illustration of cell, chromosomes: 72269964. Retrieved from https://www.dreamstime.com/stock-illustration-human-cell-chromosome-telomere-repeating-sequence-double-stranded-dna-located-ends-chromosomes-each-time-image72269964. 2016, May 31

84) Valadares, A.L., Machado, V.S., Costa-Paiva, L.S., de Sousa, M.H. and Pinto-Neto, A.M. Factors associated with the age of the onset of diabetes in women aged 50 years or more: a population-based study. *British Medical Journal open*, 4(11): e004838, 2014.

85) Diez Roux, A.V., Ranjit, N., Jenny, N.S., Shea, S., Cushman, M., Fitzpatrick, A. and Seeman, T. Race/ethnicity and telomere length in the Multi-Ethnic Study of Atherosclerosis. *Aging cell*, 8(3): 251-257, 2009.

86) Martin-Ruiz, C., Dickinson, H.O., Keys, B., Rowan, E., Kenny, R.A. and Von Zglinicki, T. Telomere length predicts poststroke mortality, dementia, and cognitive decline. *Annals of neurology*, 60(2): 174-180, 2006.

87) Muzumdar, R. and Atzmon, G. Telomere length and aging. *INTECH Open Access Publisher*, 2012.

88) O'Donovan, A., Epel, E., Lin, J., Wolkowitz, O., Cohen, B., Maguen, S., ... and Neylan, T.C. Childhood trauma associated with short leukocyte telomere length in posttraumatic stress disorder. *Biological psychiatry*, 70(5): 465-471, 2011.

89) Jiao, M.U. and Wei, L.X. Telomere and telomerase in oncology. *Cell Research*, 12(1): 1-7, 2002.

90) von Zglinicki, T. Oxidative stress shortens telomeres. *Trends in biochemical sciences*, 27(7): 339-344, 2002.

91) Cassidy, A., De Vivo, I., Liu, Y., Han, J., Prescott, J., Hunter, D.J. and Rimm, E.B. Associations between diet, lifestyle factors, and telomere length in women. *The American journal of clinical nutrition*, ajcn-28947, 2010.

92) Montpetit, A.J., Alhareeri, A.A., Montpetit, M., Starkweather, A.R., Elmore, L.W., Filler, K., ... and Collins, J.B. Telomere length: a review of methods for measurement. *Nursing research*, 63(4): 289, 2014.

93) Lin, K.W. and Yan, J. The telomere length dynamic and methods of its assessment. *Journal of cellular and molecular medicine*, 9(4): 977-989, 2005.

94) Chai, W., Du, Q., Shay, J.W. and Wright, W.E. Human telomeres have different overhang sizes at leading versus lagging strands. *Molecular cell*, 21(3): 427-435, 2006.

95) Kimura, M., Stone, R.C., Hunt, S.C., Skurnick, J., Lu, X., Cao, X., ... and Aviv, A. Measurement of telomere length by the Southern blot analysis of terminal restriction fragment lengths. *Nature protocols*, 5(9): 1596-1607, 2010.

96) Allshire, R.C., Dempster, M. and Hastie, N.D. Human telomeres contain at least three types of G–rich repeat distributed non-randomly. *Nucleic acids research*, 17(12): 4611-4627, 1989.

97) Cawthon, R.M. Telomere measurement by quantitative PCR. *Nucleic acids research*, 30(10): e47-e47, 2002.

98) Thomas, P., O'Callaghan, N.J. and Fenech, M. Telomere length in white blood cells, buccal cells and brain tissue and its variation with ageing and Alzheimer's disease. *Mechanisms of ageing and development*, 129(4): 183-190, 2008.

99) Britt-Compton, B., Rowson, J., Locke, M., Mackenzie, I., Kipling, D. and Baird, D.M. Structural stability and chromosome-specific telomere length is governed by cis-acting determinants in humans. *Human molecular genetics*, 15(5): 725-733, 2006.

100) Bendix, L., Horn, P.B., Jensen, U.B., Rubelj, I. and Kolvraa, S. The load of short telomeres, estimated by a new method, Universal STELA, correlates with number of senescent cells. *Aging cell*, 9(3): 383-397, 2010.

101) Canela, A., Vera, E., Klatt, P. and Blasco, M.A. High-throughput telomere length quantification by FISH and its application to human population studies. *Proceedings of the National Academy of Sciences*, 104(13): 5300-5305, 2007.

102) Krejci, K. and Koch, J. Improved detection and comparative sizing of human chromosomal telomeres in situ. *Chromosoma*, 107(3): 198-203, 1998.

103) Lansdorp, P.M., Verwoerd, N.P., Van De Rijke, F.M., Dragowska, V., Little, M.T., Dirks, R.W., ... and Tanke, H.J. Heterogeneity in telomere length of human chromosomes. *Human molecular genetics*, 5(5): 685-691, 1996.

104) Egholm, M., Buchardt, O., Christensen, L., Behrens, C., Freier, S.M., Driver, D. A., ... and Nielsen, P.E. PNA hybridizes to complementary oligonucleotides obeying the Watson-Crick hydrogen-bonding rules. *Nature*, 365(6446): 566, 1993.

105) Goldman, F.D., Aubert, G., Klingelhutz, A.J., Hills, M., Cooper, S.R., Hamilton, W.S., ... and Lansdorp, P.M. Characterization of primitive hematopoietic cells from patients with dyskeratosis congenita. *Blood*, 111(9): 4523-4531, 2008.

106) Artandi, S.E., Chang, S., Lee, S. L., Alson, S., Gottlieb, G.J., Chin, L. and DePinho, R.A. Telomere dysfunction promotes non-reciprocal translocations and epithelial cancers in mice. *Nature*, 406(6796): 641-645, 2000.

107) Aubert, G., Hills, M. and Lansdorp, P.M. Telomere length measurement - Caveats and a critical assessment of the available technologies and tools. *Mutation Research/Fundamental and Molecular Mechanisms of Mutagenesis*, 730(1): 59-67, 2012.

108) Vera, E. and Blasco, M.A. Beyond average: Potential for measurement of short telomeres. *Aging*, 4: 379-392, 2012.

109) Baerlocher, G.M., Vulto, I., De Jong, G. and Lansdorp, P.M. Flow cytometry and FISH to measure the average length of telomeres (flow FISH). *Nature protocols*, 1(5): 2365-2376, 206.

110) Hultdin, M., Grönlund, E., Norrback, K.F., Eriksson-Lindström, E., Roos, G. and Just, T. Telomere analysis by fluorescence in situ hybridization and flow cytometry. *Nucleic acids research*, 26(16): 3651-3656, 1998.

111) Alter, B.P., Baerlocher, G.M., Savage, S.A., Chanock, S.J., Weksler, B.B., Willner, J.P. and Lansdorp, P.M. Very short telomere length by flow fluorescence in situ hybridization identifies patients with dyskeratosis congenita. *Blood*, 110: 1439-1447, 2007.

112) Samassekou, O., Gadji, M., Drouin, R. and Yan, J. Sizing the ends: normal length of human telomeres. *Annals of Anatomy-Anatomischer Anzeiger*, 192(5): 284-291, 2010.

113) Therkelsen, A.J., Nielsen, A., Koch, J., Hindkjaer, J., Kølvraa, S. Staining of human telomeres with primed in situ labeling (PRINS). *Cytogenetic and Genome Research*, 68: 115-118, 1995.

114) Nakamura, Y., Hirose, M., Matsuo, H., Tsuyama, N., Kamisango, K. and Ide, T. Simple, rapid, quantitative, and sensitive detection of telomere repeats in cell lysate by a hybridization protection assay. *Clinical chemistry*, 45(10): 1718-1724, 1999.

115) Cimino-Reale, G., Pascale, E., Battiloro, E., Starace, G., Verna, R. and D'Ambrosio, E. The length of telomeric G-rich strand 3′-overhang measured by oligonucleotide ligation assay. *Nucleic acids research*, 29(7): e35-e35, 2001.

116) Tahara, H., Kusunoki, M., Yamanaka, Y., Matsumura, S. and Ide, T. G-tail telomere HPA: simple measurement of human single-stranded telomeric overhangs. *Nature methods*, 2(11): 829-831, 2005.

117) Wright, W.E., Tesmer, V.M., Huffman, K.E., Levene, S.D. and Shay, J.W. Normal human chromosomes have long G-rich telomeric overhangs at one end. *Genes and development*, 11(21): 2801-2809, 1997.

118) Zhao, Y., Hoshiyama, H., Shay, J. W. and Wright, W.E. Quantitative telomeric overhang determination using a double-strand specific nuclease. *Nucleic acids research*, 36(3): e14, 2008.

119) Chinta, S.J., Woods, G., Rane, A., Demaria, M., Campisi, J. and Andersen, J.K. Cellular senescence and the aging brain. *Experimental Gerontology*, 68, 3-7, 2015.

120) Meyerson, M., Counter, C.M., Eaton, E.N., Ellisen, L.W., Steiner, P., Caddle, S. D., ... and Bacchetti, S. hEST2, the putative human telomerase catalytic subunit gene, is up-regulated in tumor cells and during immortalization. *Cell*, 90(4): 785-795, 1997.

121) Holohan, B., De Meyer, T., Batten, K., Mangino, M., Hunt, S.C., Bekaert, S., ... and Shay, J. W. Decreasing initial telomere length in humans intergenerationally understates age-associated telomere shortening. *Aging Cell*, 14(4): 669-677, 2015.

122) Olovnikov, A. M. A theory of marginotomy. *J. Theor. BioL*, 41, 181-190, 1973.

123) Harley, C. B., Vaziri, H., Counter, C. M., & Allsopp, R. C. The telomere hypothesis of cellular aging. *Experimental gerontology,* 27(4): 375-382, 1992.

124) Harley, C. B., Futcher, A. B., & Greider, C. W. Telomeres shorten during ageing of human fibroblasts. *Nature*: 345(6274), 458.1990

125) Lingner, J., Hughes, T. R., Shevchenko, A., Mann, M., Lundblad, V., & Cech, T. R. Reverse transcriptase motifs in the catalytic subunit of telomerase. *Science*: 276(5312), 561-567. 1997

126) Harrington, L., Zhou, W., McPhail, T., Oulton, R., Yeung, D. S., Mar, V., ... & Robinson, M. O. Human telomerase contains evolutionarily conserved catalytic and structural subunits. *Genes & development*: 11(23), 3109-3115. 1997

Appendix A: Sample Calculations

Determining how much double distilled H_2O is required to dilute the purified DNA sample to 5 ng/µL

Final volume for the qPCR - ready purified DNA solution = (20 µL (arbitrary starting volume) x the concentration determined from the Quantus fluorometer)/(5 ng/µL (known concentration needed for the qPCR))

Amount of double distilled water to add to purified DNA solution (to achieve a concentration of 5 ng/µL) = the final volume for the qPCR - ready purified DNA solution (calculated above) -20 µL (the arbitrary starting volume)

Calculations for the Starting Quantity (length) of the Telomere (Telo) standards for the lowest dilution in the dilution series (1/10,000)

The oligomer standard is 84 bp in length (TTAGGG multiplied by 14), also having a molecular weight of 26667.2 g/mol (1). The weight of one molecule is determined by dividing the molecular weight (2.6667E+04 g/mol) by Avogadro's Number (6.02E+23 mol) = **0.44×10^{-19} g.**

A 1/10 dilution of the telo standard has a mass of 349.33 ng/µL. Multiply this value by 4 µL (the amount of sample used in each PCR reaction) to get **1397.32 g** per reaction. Divide this number by 1000 to get the mass per reaction for a 1/10,000 dilution (the highest concentration in dilution series). This equates to **1.39732 g** per reaction. To put the units into picograms per reaction, this value is multiplied by 1000, giving **1,397,32 pg** per reaction.

Therefore, there are **1,397,32 pg/0.44E-19 = 3.15436E10** molecules of oligomer in the telo standard.

The amount of telomere sequence in the telo standard is calculated: **3.15436E10** × 84 /(oligomer length) = **2.6497E06.** This is then divided by 1000 to give the value in kb in the 1/10,000 serial dilution: ***2.6497E09 kb***

Calculations for the Starting Quantity (length) of the 36B4 standards for the lowest dilution in the dilution series (1/10)

The synthesised 36B4 oligomer standard is 75 bp in length with a MW of 23268.1 g/mol.
The weight of one molecule is the molecular weight divided by Avogadro's number. The mass of the of the 36B4 oligomer standard is: (2.32681E+04 g/mol)/(6.02E+23 mol) =
0.38 × 10-19 g.

The highest concentration standard (SCG STD A) had (360.00ng/µL *4 µL = **1440 ng**)
of the 36B4 oligomer standard for a 1/10 dilution. This is equivalent to **1440 pg** per reaction for a 1/10,000 dilution.

Therefore, there are (**1440E-12 g**)/ (**0.38E-19**) = **3.7256E10** copies of the 36B4 amplicon in the 36B4 standard. Divide this value by 2 to get **1.86282E10** diploid genome copies for the 1/10,000 dilution

This value is divided by two since the standard has a diploid genome copy, giving 1.9156E+12.

This value is then multiplied by 75 base pairs to give: **1.4367E+14 kb.**

The rest of the standard dilution is known as well

Appendix B: Information Used in qPCR Set-up

Table 13: Information of the standards and primers used for the qPCR amplification (35)

	Oligomer Name	Species	Oligomer sequence (5′-3′)	Amplicon size
Standards	Telomere standard	Human/rodent	(TTAGGG)14	**84 bp**
	36B4 standard	Human	CAGCAAGTGGGAAGGTGTAATCCGTCTCCACAGACAAGGCCAGGACTCGTTTG TACCCGTTGATGATAGAATGGG	**75 bp**
PCR Primers	teloF	Human/rodent	CGGTTTGTTTGGGTTTGGGTTTGGGTTTGGG TTTGGGTT	**>76 bp**
	teloR	Human/rodent	GGCTTGCCTTACCCTTACCCTTACCC TTACCCTTACCCT	

Table 14 The contents of each qPCR amplification reaction (35)

Reagents	Volumes for one sample (ul)	Final concentration
Power SYBR Green master mix (2x)	10	1x
Primer (telomere-fwd (2 μM))	1	0.1 μM
Primer telomere-rev (2 μM)	1	0.1 μM
H_20	4	
DNA (5 ng/μl DNA)	4	20 ng total

Appendix C: Analyzing qPCR Amplification Curves and Determining Average Absolute Telomere Length

Eighteen qPCR amplifications were required to obtain all the data for this study. Including all eighteen amplification curves, standard curve calculations, standard curves, and final calculations would be quite cumbersome and rather inefficient, a sample of only one qPCR amplification is included here for reference. All eighteen amplifications were processed identically to the one shown here, and the resultant data from all amplifications can be found in Table 1.

Below is the amplification curve (Figure 8). The CFX manager software was used to analyze the qPCR data and it measure the amount of amplification cycles which crossed a predetermined threshold level of reflective fluorescent units (RFUs). This generates a value known as Cq, which is analogous to the cycle threshold (Ct).

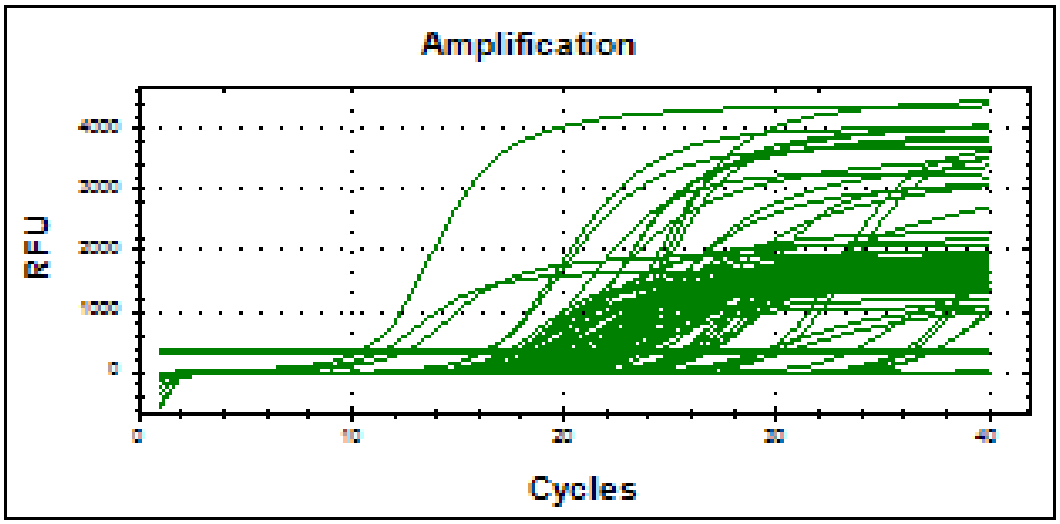

Figure 7: A sample of amplification curves from the qPCR amplification reaction run with a Biorad Real Time System C1000 Thermocycler, detected with a CFX96 Optics Module, and tabulated via the CFX Manager software.

The known concentrations of the telomere standards are plotted alongside the resultant Cq values obtained from the CFX Manager Software to create a telomere length standard curve with a known slope (Table 8, Figure 9).

Table 15: Resultant qPCR data and nucleic acid quantification data needed to construct a telomere standard curve.

Telomere standard serial dilution	Average concentration of standard (ng/uL)	Telomere length (kb)	LOG telomere length (kb)	Cq Average
100K	0.001217	9293454.5	6.968177179	22.94
1M	0.0001217	929345.45	5.968177179	26.04
10M	0.00001217	92934.545	4.968177179	29.615

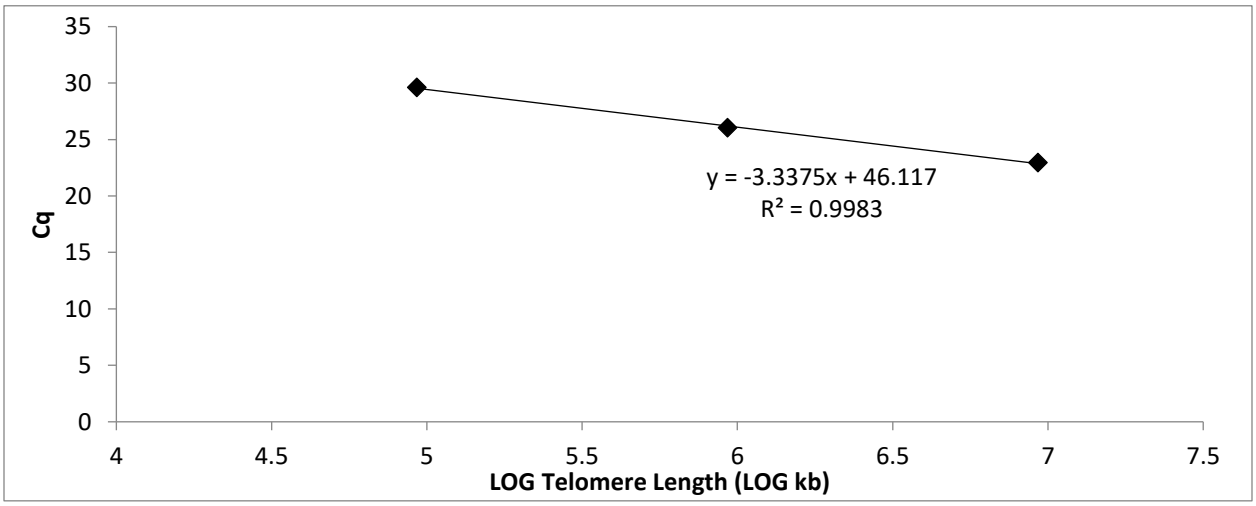

Figure 8: The resultant standard curve obtained from the LOG quantity of telomeres and the Cq values (Table 15). The equation of the line is y = -3.337x + 46.11 and the r^2 value is 0.998.

Similarly, the known concentrations of the 36B4 standards are plotted alongside the resultant Cq values obtained from the CFX Manager Software to create a (single genome copy standard curve with a known slope (Table 9, Figure 10).

Table 16: Resultant qPCR data and nucleic acid quantification data needed to construct a single gene copy standard curve.

36B4 standard serial dilution	Average Concentration of Standard (ng/uL)	single genome copies	LOG single Genome Copies	Cq average:
100K	0.00066	34736842	7.540790335	11.267
1M	0.000066	3473684.2	6.540790335	17.507
10M	0.0000066	347368.42	5.540790335	20.483

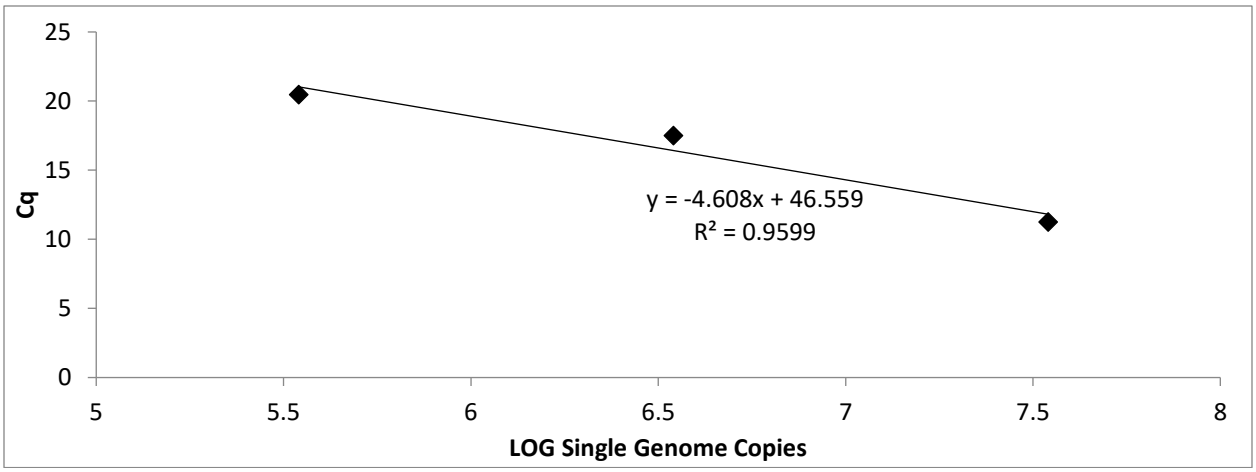

Figure 9: The resultant standard curve obtained from the LOG quantity of telomeres and the Cq values (Table 16). The equation of the line is y = -4.608x + 46.55 and the r^2 value is 0.959.

Lastly, the unknown samples that were amplified are tested. The sample have their Cq values compared to each standard curve, with the samples amplified using telomere primers compared to the telomere standard curve and the samples amplified using 36B4 primers compared to the single genome copy standard curve. For this, the log (telomere length (kb)) and log (single genome copies) can be calculated. The antilog function can be used convert to units of telomere length (kb) and single genome copies. The absolute telomere length per genome can be determined by dividing the calculated telomere length (kb) by the number of single genome copies. This number can be divided by 46 to obtain the average absolute telomere length per chromosome (See Table below for how this can be completed)

Table 17: Data required for the calculation of the absolute telomere length genome (kb/genome) and Average Absolute Telomere Length per chromosome (kb/chromosome)

Sample	CQ Value for samples treated with telomere primers	CQ Value for samples treated with 36B4 primers	LOG telomere length (kb)	LOG single genome copies	Telomere length (kb)	36B4 (single genome copies)	Absolute telomere length/ genome (kb/genome)	Average absolute telomere length/ chromosome (kb/chromosome)
36	20.33	23.1	7.72550195	5.088975694	53149838.3	122737.0539	433.0382444	9.413874879
67	17.727	19.665	8.5055439	5.834418403	320290385	682996.3815	468.9488756	10.19454077
40	19.257	21.665	8.04704825	5.400390625	111441833	251414.6757	443.2590608	9.636066539
49	16.155	21.2	8.97662571	5.501302083	947601439	317177.2894	2987.608101	64.9480022
46	19.247	22.187	8.05004495	5.287109375	112213459	193690.9704	579.3427487	12.59440758
10	18.63	22.15	8.23494156	5.295138889	171767725	197305.3625	870.5679517	18.92539025
7	23.047	25.387	6.91129757	4.592664931	8152627	39143.97547	208.2728414	4.527670466
28	21.49	20.133	7.37788433	5.732855903	23871753.8	540574.9325	44.1599349	0.959998585
72	28.667	22.173	5.22715013	5.290147569	168713.616	195050.7252	0.864973028	0.018803761